Inorganic Chemistry

Article

pubs.acs.org/IC

Effect of the Phosphine Steric and Electronic Profile on the Rh-Promoted Dehydrocoupling of Phosphine–Boranes

Thomas N. Hooper,[†] Miguel A. Huertos,[†] Titel Jurca,[‡] Sebastian D. Pike,[†] Andrew S. Weller,*[,†] and Ian Manners[‡]

[†]Department of Chemistry, University of Oxford, Mansfield Road, Oxford OX1 3TA, United Kingdom

[‡]School of Chemistry, University of Bristol, Cantock's Close, Bristol BS8 1TS, United Kingdom

Supporting Information

ABSTRACT: The electronic and steric effects in the stoichiometric dehydrocoupling of secondary and primary phosphine–boranes $H_3B{\cdot}PR_2H$ [R = 3,5-$(CF_3)_2C_6H_3$; *p*-$(CF_3)C_6H_4$; *p*-$(OMe)C_6H_4$; adamantyl, Ad] and $H_3B{\cdot}PCyH_2$ to form the metal-bound linear diboraphosphines $H_3B{\cdot}PR_2BH_2{\cdot}PR_2H$ and $H_3B{\cdot}PRHBH_2{\cdot}PRH_2$, respectively, are reported. Reaction of $[Rh(L)(\eta^6\text{-}FC_6H_5)][BAr^F{}_4]$ [L = $Ph_2P(CH_2)_3PPh_2$, Ar^F = 3,5-$(CF_3)_2C_6H_3$] with 2 equiv of $H_3B{\cdot}PR_2H$ affords $[Rh(L)(H)(\sigma,\eta\text{-}PR_2BH_3)(\eta^1\text{-}H_3B{\cdot}PR_2H)][BAr^F{}_4]$. These complexes undergo dehydrocoupling to give the diboraphosphine complexes $[Rh(L)(H)(\sigma,\eta^2\text{-}PR_2{\cdot}BH_2PR_2{\cdot}BH_3)][BAr^F{}_4]$. With electron-withdrawing groups on the phosphine–borane there is the parallel formation of the products of B–P cleavage, $[Rh(L)(PR_2H)_2][BAr^F{}_4]$, while with electron-donating groups no parallel product is formed. For the bulky, electron rich, $H_3B{\cdot}P(Ad)_2H$ no dehydrocoupling is observed, but an intermediate Rh(I) σ phosphine–borane complex is formed, $[Rh(L)\{\eta^2\text{-}H_3B{\cdot}P(Ad)_2H\}][BAr^F{}_4]$, that undergoes B–P bond cleavage to give $[Rh(L)\{\eta^1\text{-}H_3B{\cdot}P(Ad)_2H\}\{P(Ad)_2H\}][BAr^F{}_4]$. The relative rates of dehydrocoupling of $H_3B{\cdot}PR_2H$ (R = aryl) show that increasingly electron-withdrawing substituents result in faster dehydrocoupling, but also suffer from the formation of the parallel product resulting from P–B bond cleavage. $H_3B{\cdot}PCyH_2$ undergoes a similar dehydrocoupling process, and gives a mixture of stereoisomers of the resulting metal-bound diboraphosphine that arise from activation of the prochiral P–H bonds, with one stereoisomer favored. This diastereomeric mixture may also be biased by use of a chiral phosphine ligand. The selectivity and efficiencies of resulting catalytic dehydrocoupling processes are also briefly discussed.

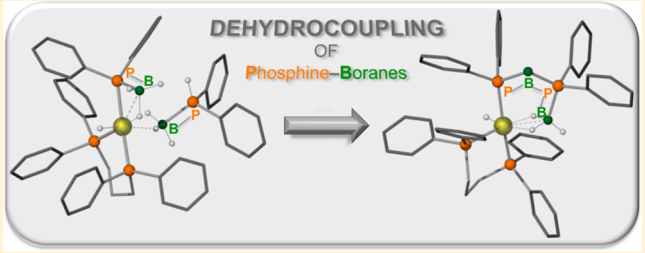

INTRODUCTION

The development of efficient catalytic methods for the formation of bonds between main group elements is of considerable interest for the continued development of main group chemistry. Such processes enable new discoveries to be made in the promising application areas that main group species are now occupying, such as high performance polymers, emissive materials, etch resists for lithography, and precursors to ceramic thin films or devices.[1−6] However, the development of this field lags substantially behind the advances made in catalytic C–C and C–X bond formation, for which there are now a myriad of efficient ways to promote such unions that are important for the construction of new molecules. Catalytic dehydrocoupling[5,7,8] of amine– and phosphine–boranes is one method that has emerged for the formation of B–N and B–P bonds, and development in the area has been spurred on by the potential for ammonia–borane to act as a hydrogen carrying vector.[9−11] In addition, polymeric materials that can arise from dehydropolymerization of primary analogues are also of significant interest as they are valence isoelectronic with technologically ubiquitous polyolefins. Although the metal catalyzed formation of polyaminoboranes has attracted recent attention,[12−18] catalytic routes to polyphosphinoboranes have also been known since 1999.[19] Perhaps the best example is that of the $[Rh(COD)_2][OTf]$ catalyzed dehydrocoupling of secondary, $H_3B{\cdot}PR_2H$, and primary, $H_3B{\cdot}PRH_2$, phosphine–boranes to give oligomeric and polymeric materials (Scheme 1).[19−21]

In contrast to amine–borane dehydrocoupling,[8,10,15,22−24] the mechanism of catalytic dehydrocoupling of phosphine–

Scheme 1. Phosphine–Borane Dehydrocoupling

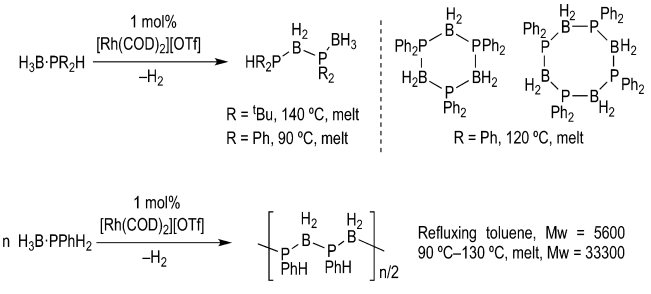

Received: January 6, 2014
Published: March 11, 2014

   dx.doi.org/10.1021/ic500032f | *Inorg. Chem.* 2014, 53, 3716–3729

Scheme 2. Proposed Catalytic Cycle for the Dehydrocoupling of $H_3B{\cdot}PR_2H$ To Give $H_3B{\cdot}PR_2BH_2{\cdot}PR_2H$[a]

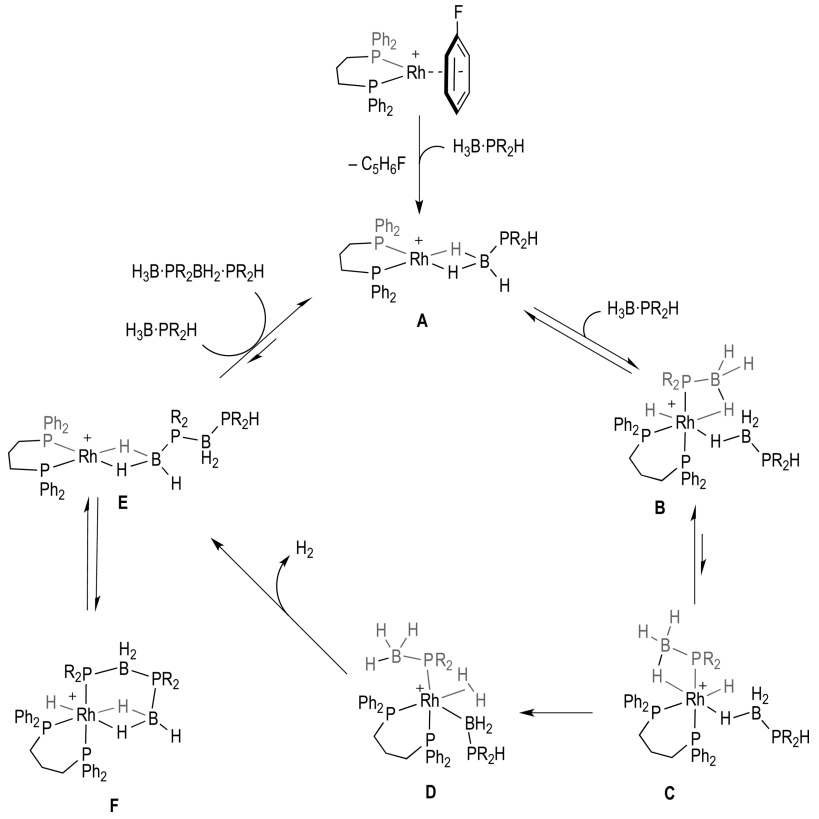

[a] $[BAr^F{}_4]^-$ anions are not shown.

boranes has received less attention. Although initial reports demonstrated that catalysis using $[Rh(COD)_2][OTf]$ was a homogeneous process (i.e., not colloidal),[25] there has been only sporadic further work on elucidating the mechanistic details.[26−29] Progress has no doubt been slowed due to the fact that the reaction conditions reported for phosphine−borane dehydrocoupling often require melt conditions, thus making interrogation of the catalytic cycle problematic. Recently, we have reported that the Rh(I) complexes $[Rh(P^tBu_2H)_2(\eta^6\text{-}FC_6H_5)][BAr^F{}_4]$,[30] and $[Rh(L)(\eta^6\text{-}FC_6H_5)][BAr^F{}_4]$,[31] [L = $Ph_2P(CH_2)_3PPh_2$] are particularly well-suited to the study of the dehydrocoupling mechanism of secondary phosphine−boranes in solvents such as fluorobenzene; and on the basis of the observation of intermediates, kinetic studies, and H/D exchange experiments we have proposed a catalytic cycle for the dehydrocoupling of $H_3B{\cdot}PR_2H$ (R= Ph, ^{t}Bu; Scheme 2). For this cycle, intermediate species were isolated, but their structures could not be confirmed by X-ray crystallography. In particular for R = Ph, a β-B-agostic σ complex **B**, and the product of dehydrocoupling **F**, that is proposed to sit off cycle, could be isolated and spectroscopically characterized. Under stoichiometric conditions the observation that **B** transforms into **F** on gentle heating allowed for kinetic parameters to be determined that suggested that the rate-determining step(s) for dehydrocoupling were located within the transformations **B** to **D**. In solution phase the turnover limiting step for catalysis is proposed to be the displacement of the linear diboraphosphine product (i.e., **F** to **A**), although under the melt conditions used for efficient catalysis this may well be different. Further insight comes from the observations that for R = ^{t}Bu the barrier to dehydrocoupling is higher (70 °C versus 25 °C for reaction), P−H activation appears also to be a higher energy process, different intermediates (**A** and **E**) are observed, and the turnover limiting process in catalysis is now suggested to be the P−H activation/dehydrocoupling steps. Prior work has demonstrated a similar difference in relative rates of dehydrocoupling of secondary $H_3B{\cdot}PR_2H$ [R = p-$(CF_3)C_6H_4$, Ph, ^{t}Bu, ^{i}Bu] and primary $H_3B{\cdot}PRH_2$ [R = Ph, ^{t}Bu, ^{i}Bu] phosphine−boranes using the $[Rh(COD)_2][OTf]$ catalyst, and this was suggested to be due to a combination of steric and electronic (relative P−H bond strengths) factors,[21,32,33] although the mechanism of dehydrocoupling of phosphine−boranes using this catalyst is currently not known.[20,25,30] Interestingly, the related dehydrogenation of aryl amine−boranes shows that the activity of the N−H bond is such that spontaneous dehydrocoupling occurs in the absence of catalyst, with electron-withdrawing aryl groups [p-$(CF_3)C_6H_4$] undergoing faster reaction than electron-donating [p-$(OMe)C_6H_4$].[34] Very recent work has shown that paramagnetic Ti(III) centers might also be involved in dehydrocoupling of phosphine− and amine−boranes when using Cp_2Ti-based catalysts,[35] while oligomerization of base-stabilized phosphino−boranes at Cp_2Ti centers has been described.[29] Likely decomposition routes in Rh-systems for phosphine−borane dehydrocoupling to form bis(phosphine)boronium salts have also recently been discussed.[36]

In this Article, we report an extension of our investigations into the mechanism of phosphine−borane dehydrocoupling using the $\{Rh(Ph_2P(CH_2)_3PPh_2)\}^+$ fragment, by varying the electronic and steric profile of the secondary phosphine−boranes $H_3B{\cdot}PR_2H$ [R = 3,5-$(CF_3)_2C_6H_3$; p-$(CF_3)C_6H_4$; p-$(OMe)C_6H_4$; adamantyl], as well as investigations with the

dx.doi.org/10.1021/ic500032f | Inorg. Chem. 2014, 53, 3716−3729

primary phosphine–borane $H_3B{\cdot}PCyH_2$. Dehydrocoupling forms the corresponding metal–bound linear diboraphosphines $H_3B{\cdot}PR_2BH_2{\cdot}PR_2H$ and $H_3B{\cdot}PRHBH_2{\cdot}PRH_2$, respectively. These studies provide insight into the determining role of the electronics and sterics of the phosphine–borane in the dehydrocoupling process, as well as providing as yet unreported examples of the solid-state structures of the intermediates related to the catalytic cycle. We also report for the first time the partial control of diastereoselectivity in dehydrocoupling of primary phosphine–boranes, that can additionally be biased by use of a chiral chelating phosphine on the rhodium center.

RESULTS AND DISCUSSION

Phosphine–Borane and Diboraphosphine Starting Materials. A range of secondary phosphine–boranes with differing electronic and steric properties have been used in this study (**1**, **2**, **3**, and **4**, Figure 1), which also provide comparison

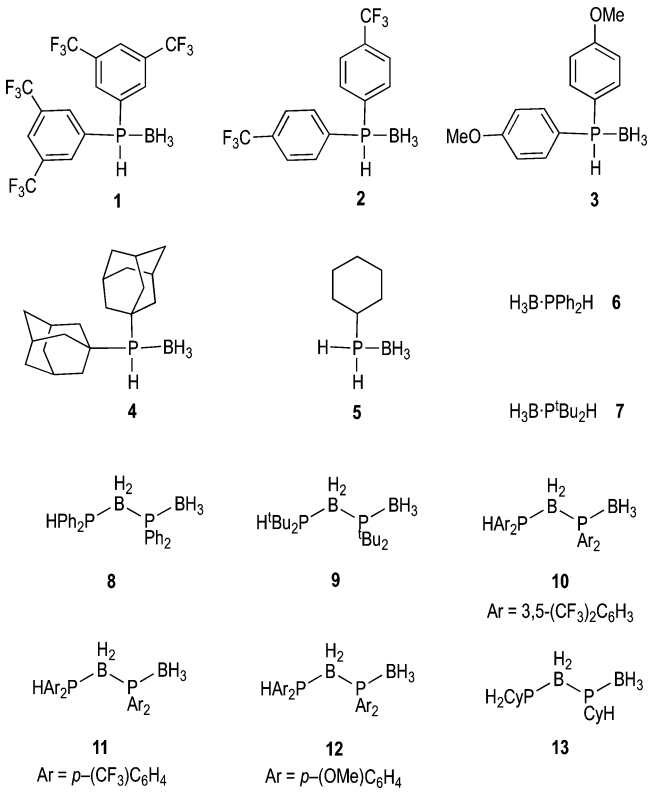

Figure 1. Phosphine–boranes **1**–**7** and diboraphosphines **8**–**13**.

with the previously reported Ph, **6**, and ^{t}Bu, **7**, analogues.[31] The primary phosphine–borane **5** has also been used.[37] Compounds **2**[33] and **3**[38] are known adducts and offer electron-withdrawing and donating aryl groups, respectively. Bis-CF_3-substituted **1** is a new complex and offers an alternative to **2**. The synthesis of adamantyl-substituted phosphine, **4**, an analogue of **7**, has been reported in the patent literature.[39] Compared with the ^{t}Butyl group, adamantyl has a greater steric bulk due to its larger volume and rigid structure.[40,41] The new linear diboraphosphines, **10**–**13**, have also been synthesized to aid in the identification of final dehydrocoupling products. Complexes **10**–**12** are synthesized by a Rh-catalyzed process from the corresponding phosphine–boranes, while primary phosphine containing **13** has been synthesized in good isolated yield (85%) by addition of $[NBu_4][BH_4]$ to the bis-(phopshine)boronium $[(CyH_2P)_2BH_2]Br$.[36]

Stoichiometric Dehydrocoupling of Secondary Phosphine–Boranes. Addition of 2 equiv of **1** to $[Rh(L)(\eta^6\text{-}FC_6H_5)][BAr^F{}_4]$ [L = $Ph_2P(CH_2)_3PPh_2$] in 1,2-$F_2C_6H_4$ solution at 25 °C rapidly (on time of mixing) resulted in the formation of $[Rh(L)(H)(\sigma,\eta\text{-}PR_2BH_3)(\eta^1\text{-}H_3B{\cdot}PR_2H)][BAr^F{}_4]$, **14** [R = 3,5-$(CF_3)_2(C_6H_3)$, Scheme 3], which was

Scheme 3. Synthesis of Complexes 14, 15, and 16[a]

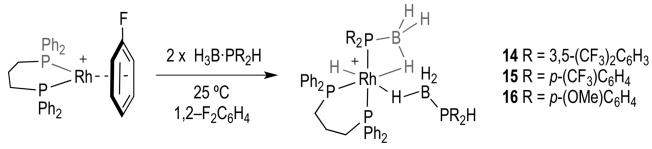

[a] $[BAr^F{}_4]^-$ anions are not shown.

characterized by NMR spectroscopy, ESI-MS (electrospray ionization mass spectrometry), and single crystal X-ray diffraction. Likewise, the use of 2 equiv of phosphine–borane **2** or **3** results in the formation of the analogous complexes **15** [R = *p*-$(CF_3)C_6H_4$] and **16** [R = *p*-$(OMe)C_6H_4$], respectively, which were fully characterized using solution techniques. All these complexes proceed to dehydrocouple (vide infra), and only for **14** was an analytically pure crystalline solid obtained. Even so, dissolution of crystalline material of **14** resulted in the observation of small amounts (approximately 5–10%) of the associated dehydrocoupling product in the solution NMR spectra after short periods of time. Complexes **15** and **16** could only be isolated as oils, but their characterization by NMR spectroscopy and ESI-MS was fully consistent with their formulation.

The solution NMR spectra for **14**, **15**, and **16** are very similar to those previously reported for $[Rh(L)(H)(\sigma,\eta\text{-}PPh_2BH_3)(\eta^1\text{-}H_3B{\cdot}PPh_2H)][BAr^F{}_4]$ (i.e., **B**, Scheme 2[31]), and data for **14** is discussed in detail. The $^{31}P\{^1H\}$ NMR spectrum of **14** shows four different phosphorus environments. Two of the resonances are broadened significantly compared to the other two, suggesting these phosphorus atoms are bound to a quadrupolar boron center. One of these shows both a large *trans* PP coupling [J(PP) 244 Hz] and coupling to ^{103}Rh [J(RhP) 75 Hz], while the other is a broad singlet. The other two signals are sharper and are assigned to the two ^{31}P environments of the $Ph_2P(CH_2)_3PPh_2$ ligand. One of these sharper resonances [δ 29.5, ddd, J(RhP) 130, J(PP) 35, J(PP) 21 Hz] is assigned to the phosphorus atom *trans* to the weakly bound β-B-agostic interaction on the basis of the larger ^{103}Rh coupling constant, while the other signal [δ 11.3, ddd, J(RhP) 103, J(PP) 244, J(PP) 35 Hz] is assigned to the phosphorus atom *trans* to the coordinated phosphido ligand. In the ^{1}H NMR spectrum of **14** one broad, relative integral 3H, signal is observed at δ −0.78, indicative of a Rh···H_3B σ interaction in which the B–H bonds are undergoing rapid site exchange on the NMR spectroscopic time scale between terminal and bridging sites.[42] A broad, relative integral 1H, resonance at δ −6.12 is assigned to a static β-B-agostic B–H interaction. Cooling of the solution to 0 °C led to the resolution of this signal as doublet [J(PH) = 65 Hz], fully consistent with its *trans* disposition to a phosphine. The remaining BH(terminal) signals are not observed, and it is likely they are coincident with the $\{CH_2\}_3$ signals. A sharper signal at δ −16.21, relative integral 1H, is assigned to a metal–hydride resonance, in which the coupling to both ^{103}Rh and ^{31}P

dx.doi.org/10.1021/ic500032f | Inorg. Chem. 2014, 53, 3716–3729

is clearly small and unresolved. The PH group is observed at δ 5.81 that collapses into a singlet in the $^{1}H\{^{31}P\}$ NMR spectrum. The ^{11}B NMR spectrum shows a broad signal centered at δ −39.8, which is not shifted significantly from that of free phosphine−borane **1** (δ −42.0). This is assigned to a coincidence of the η^1 β-*B*−H···Rh agostic and σ Rh···H_3B signals, as has been noted previously.[31,43] Complexes **15** and **16** have similar ^{1}H, ^{11}B, and ^{31}P NMR spectra, and thus we assign very similar structures.

Crystals of complex **14** of suitable quality for analysis by X-ray diffraction were obtained by layering of a 1,2-$F_2C_6H_4$ solution with pentane at −26 °C. The structure of **14** in the solid-state (Figure 2) is fully consistent with the structure

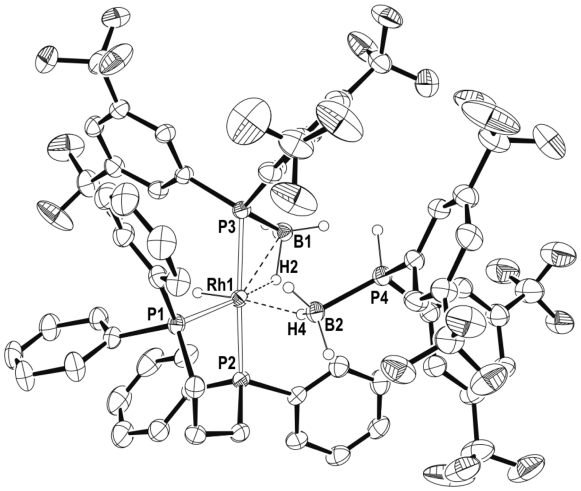

Figure 2. Molecular structure of the cation of **14**. Displacement ellipsoids are drawn at 50% probability level. Some hydrogen atoms are omitted for clarity. Selected bond lengths (Å) and angles (deg): Rh1−P1, 2.778(10); Rh1−P2, 2.3163(9); Rh1−P3, 2.3045(10); P3−B1, 1.913(4); P4−B2, 1.918(4); Rh1···B1, 2.515(4); Rh1···B2, 2.740(4); Rh1−P3−B1, 72.54(14); Rh1−B2−P4, 121.3(2).

deduced from the solution NMR spectroscopic data. The formally Rh(III) center adopts a pseudo-octahedral geometry, with the chelating phosphine ligand and the hydride located on one of the faces of the octahedron. Two of the three remaining coordination sites are occupied by a phosphine−borane unit that has undergone P−H activation, and is bound to the metal *via* a phosphido bond [Rh1−P3, 2.3045(10) Å] and a β-B-agostic bond [Rh1−B1, 2.515(4) Å]. The other phosphine−borane unit occupies the last coordination site *via* a σ η^1-Rh···H−B interaction.[42] All the hydrides (B−H and Rh−H) were located in the final difference map. The structure is in full accord with the solution NMR spectroscopic data, confirming the spectroscopic assignments that have been made previously.[31] β-B-agostic interactions are known,[35,44,45] and we have recently reported $[Rh(\kappa^1,\eta\text{-}PPh_2BH_2{\cdot}PPh_3)(PPh_3)_2][BAr^F{}_4]$ in which a base-stabilized phosphine−borane adopts a β-B-agostic interaction with the Rh-center.[36] σ phosphine−boranes are also known,[42,46,47] and bimetallic complexes showing both B-agostic and σ borane coordination modes have been reported.[48] Compared to a Rh(I) complex that shows a bidentate η^2-coordination mode for the σ borane, $[Rh(P^tBu_2H)_2(\eta^2\text{-}H_3B{\cdot}P^tBu_2H)][BAr^F{}_4]$,[30] the Rh···B distance for the η^1-interaction in **14** is considerably longer [2.188(3) Å versus 2.740(4) Å, respectively], consistent with this different binding motif. Similar changes in M···B distance have been noted on moving between η^1 and η^2 coordination modes in chelating phosphine−boranes.[43]

Complexes **14**−**16** undergo spontaneous dehydrocoupling (25 °C) to form products of the general formula $[Rh(L)H(\sigma,\eta^2\text{-}PR_2{\cdot}BH_2PR_2{\cdot}BH_3)][BAr^F{}_4]$: **17**, R = 3,5-$(CF_3)_2C_6H_3$; **18**, R = *p*-$(CF_3)C_6H_4$; **19**, R = *p*-$(OMe)C_6H_4$ (Scheme 4). This

Scheme 4. Dehydrocoupling of Complexes 14−16[a]

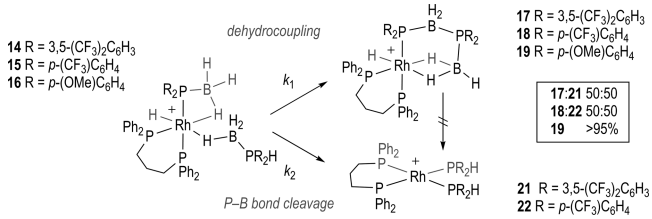

[a] $[BAr^F{}_4]^-$ anions are not shown. Time = 6 h **17**/**21**, **18**/**22** (25 °C); 8 h **16**/**19** (35 °C).

process also results in the liberation of H_2 (observed, ^{1}H NMR spectroscopy). For **17** and **18** there are additional products formed, assigned as $[Rh(L)(PR_2H)_2][BAr^F{}_4]$, **21** and **22**, respectively, on the basis of NMR spectroscopic data. These complexes are formed in parallel to **17** and **18**, as preformed **17** (*vide infra*) does not proceed to form **21**. Complex **21** has been independently prepared by addition of two equivalents of $HP((CF_3)_2C_6H_3)_2$ to $[Rh(L)(\eta^6\text{-}FC_6H_5)][BAr^F{}_4]$.

This mixture of products observed for the electron-withdrawing phosphine substituents (i.e., **1** and **2**) contrasts with that found for when R = Ph[31] and *p*-$(OMe)C_6H_4$, which yield the dehydrocoupled (e.g., **19** and **F**, Scheme 2) product in essentially quantitative form (∼95% by $^{31}P\{^{1}H\}$ NMR spectroscopy). Complex **17** has been synthesized cleanly from direct addition of the preformed dehydrocoupled diboraphosphine product, **10**, to $[Rh(L)(\eta^6\text{-}FC_6H_5)][BAr^F{}_4]$, Scheme 5. It was from this reaction that material of **17** suitable for single crystal X-ray diffraction was obtained.

Scheme 5. Synthesis of 17 by Direct Addition of the Linear Diboraphosphine 10[a]

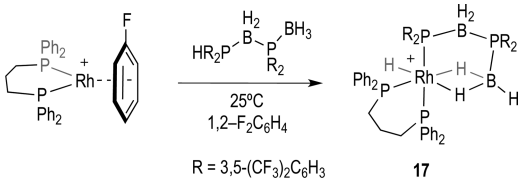

[a] $[BAr^F{}_4]^-$ anions are not shown.

Figure 3 shows the solid-state structure of **17**, in which the diboraphosphine acts as a chelate to the Rh(III) center, *via* a phosphido group and two B-agostic interactions: $[Rh(L)H(\sigma,\eta^2\text{-}PR_2{\cdot}BH_2PR_2{\cdot}BH_3)][BAr^F{}_4]$ [R = 3,5-$(CF_3)_2C_6H_3$]. All the hydride ligands (B−H and Rh−H) were located in the final difference map. The Rh(III) center has pseudo-octahedral geometry, in which the oligomeric phosphine−borane is bound tridentate to the metal through η^2-BH_2···Rh [B2−Rh1, 2.280(5) Å] and phosphido [P3−Rh1, 2.3925(10) Å] interactions. The hydride ligand is positioned *trans* to one of the B−H···Rh interactions. The Rh···B distance is considerably shorter than those observed in **14**, consistent with the η^2-bidentate binding mode of the borane. This distance is similar

dx.doi.org/10.1021/ic500032f | Inorg. Chem. 2014, 53, 3716−3729

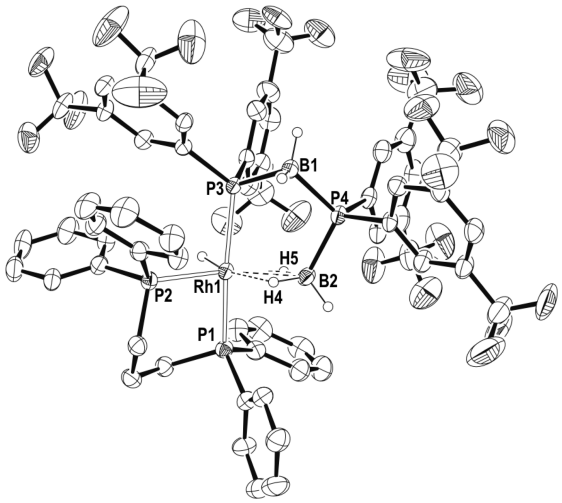

Figure 3. Molecular structure of the cation of **17**. Displacement ellipsoids are drawn at 50% probability level. Some hydrogen atoms are omitted for clarity. Selected bond lengths (Å) and angles (deg): Rh1−P1, 2.3241(11); Rh1−P2, 2.2650(11); Rh1−P3, 2.3925(10); Rh1···B2, 2.280(5); Rh1−P3−B1, 110.88(15); B1−P4−B2, 107.5(2).

to others reported for chelating phosphine−borane complexes with Rh.[49−52]

The NMR spectroscopic data for **17** are fully consistent with the solid-state structure being retained in solution and are also very similar to that reported for the analogous complex formed from the deydrocoupling of **6** (R = Ph).[31] The $^{31}P\{^{1}H\}$ NMR spectrum shows four different phosphorus environments. Two of these signals are well-resolved and show coupling to ^{103}Rh, δ 46.6 [J(RhP) 111 Hz] and δ 12.8 [J(RhP) 91 Hz], and are attributed to the chelating phosphine ligand. One of these signals (δ 12.8) also shows large $^{31}P-^{31}P$ coupling [J(PP) 260 Hz] suggesting a *trans* position relative to the phosphido center. The other two environments are broad, typical of those observed when coupling to a quadrupolar boron center. For one of these *trans* J(PP) coupling is also observed. The ^{1}H NMR spectrum shows three different broad, relative integral 1H, environments assigned to the BH_3 moiety [δ −4.54, −1.20, and 4.37]. This indicates that the BH_3 unit is not undergoing exchange on the NMR spectroscopic time scale, as noted previously for similar η^2-M···H_3B systems.[31,43,50,52] The Rh−H signal is observed at δ −13.98 as a sharper signal, although this also shows unresolved coupling. The ^{11}B NMR spectrum shows two different environments [δ −27.1 and 0.21] for the two boron atoms present in the diboraphosphine, with the latter assigned to the η^2-H_3B unit on the basis of the large downfield shift from free ligand ($\Delta\delta$ = +36.8).[43] Spectroscopic data for complexes **18** and **19**, that are produced by the direct dehydrocoupling route are similar, although for **18** this is also formed as a mixture with **22**.

The dehydrocoupling reaction (i.e., **14** to **17**) shows a dependence on the substituents on the phosphine. For electron-withdrawing aryl groups (e.g., p-CF_3), it is faster when compared with electron rich groups (i.e., p-OMe). Following these processes *in situ* using NMR spectroscopy demonstrated that these dehydrocoupling reactions follow a first order rate profile for the consumption of the starting material over at least three half-lives (see Supporting Information): **1** 3 h (25 °C); **2** 3 h (25 °C); **6** 14 h (25 °C);[31] **3** 8 h (35 °C), ∼120 h (25 °C). That the parallel products **21** and **22** are formed in approximately equal ratio to the dehydrocoupled product (**17**, **18**, respectively)) suggests that $k_1 \approx k_2$ (Scheme 4). In addition to this parallel process, direct comparison of the rate constants is further complicated by the fact that **16** → **19** required heating to 35 °C to make the reaction run over a convenient time scale for analysis by NMR spectroscopy. Nevertheless these relative rates reflect previous observations on the rate of catalytic dehydrocoupling when the electronics of a system are changed, in as much as electron-withdrawing groups promote the reaction.[21] Interestingly, for all the aryl complexes initial P−H activation to form a phosphido hydride complex (i.e., **14**) is very rapid, occurring on time of mixing. This suggests that for aryl-substituted phosphine−boranes it is not initial P−H activation that is rate-determining for the dehydrocoupling event, as we have commented on for R = Ph.[31] In this study we suggested that B−H activation/reorganization in intermediates such as **B** (Scheme 2) prior to P−B bond formation might be the rate limiting process.[31] This might well be promoted by a weaker B−H bond, and calculations on analogous $H_3B{\cdot}L$ (L = Lewis base) systems show that the B−H bond is considerably weaker when there are electron-withdrawing groups on the Lewis base.[53] However, we cannot rule out that the relative P−H bond strengths in intermediates such as **14** also might play a role, or that there is a change in the rate determining step on changing the phosphine−borane ligand, as the intimate details of the mechanism leading to P−B formation still remain to be resolved. The observation that for an electron-withdrawing phosphine there is a significant proportion of parallel product formed that results from P−B bond cleavage is consistent with the weakening of the P−B bond with increasingly electron-withdrawing aryl substiutents.[8,54] P−B bond cleavage has been noted previously in σ phosphine−borane complexes to give either simple adducts[47] or further reaction to yield bis-(phosphine)boronium salts.[30]

Prior to the formation of the parallel product **21** (R = 3,5-$(CF_3)_2C_6H_3$) an intermediate is observed that has been characterized by ^{1}H and $^{31}P\{^{1}H\}$ NMR spectroscopy as $[Rh(L)H(\sigma,\eta\text{-}PR_2{\cdot}BH_3)(PR_2H)][BAr^F{}_4]$ **20**, i.e., a complex that sits directly between **14** and **21** by loss of one "BH_3" fragment (Scheme 6). Complex **20** results from P−B bond

Scheme 6. Formation of the Parallel Products 17 and 21 from 14[a]

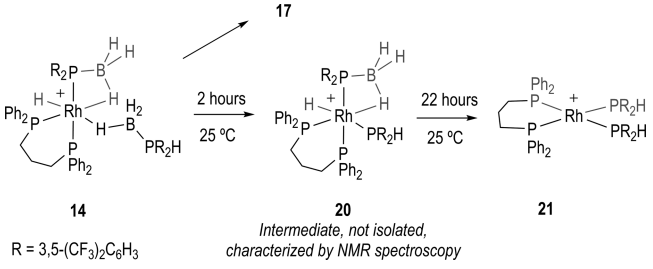

[a] $[BAr^F{}_4]^-$ anions are not shown.

cleavage, formally of the σ-$H_3B{\cdot}PR_2H$ ligand, to afford a complex with a β-B-agostic interaction from a phosphide borane ligand (as for **14**) and a simple PR_2H ligand *trans* to a hydride. Complex **20** was not isolated in pure form, being observed alongside **14** and the final products **17**/**21**. However, after 2 h reaction a significant proportion of **20** is present (∼20% by ^{31}P NMR spectroscopy), allowing for its

dx.doi.org/10.1021/ic500032f | Inorg. Chem. 2014, 53, 3716−3729

identification aided by comparison with the NMR spectroscopic data for **14** (Supporting Information). In particular four environments are observed in the ^{31}P NMR spectrum, with only one of these broadened significantly by coupling to quadrupolar boron. This signal also shows a large, mutual, *trans* J(PP) coupling with another phosphine environment. In the high-field region of the ^{1}H NMR spectrum a broad doublet is observed at δ −7.06 [J(HP) = 76 Hz] which is assigned to the β-B-agostic interaction, while there is a relatively sharper one at δ −9.61 [J(HP) = 165 Hz] assigned to Rh−H, and again ^{103}Rh coupling is not resolved. These assignments were confirmed by ^{1}H{^{31}P}, ^{1}H{^{11}B}, and ^{1}H/^{31}P correlation experiments.

Addition of 2 equiv of the bulky and electron rich phosphine−borane $H_3B{\cdot}P(adamantyl)_2H$, **4**, to $[Rh(L)(\eta^6\text{-}FC_6H_5)][BAr^F{}_4]$ in 1,2-$F_2C_6H_4$ solution at 25 °C rapidly results in a color change from orange to purple and the formation of the new σ bound Rh(I) phosphine−borane complex $[Rh(L)(\eta^2\text{-}H_3B{\cdot}P(adamantyl)_2H)][BAr^F{}_4]$, **23**, which was characterized *in situ* by NMR spectroscopy. This complex could not be isolated as it undergoes further reaction, by P−B bond cleavage at room temperature, to form **24** (Scheme 7). Addition of 1 equiv of **4** resulted in a final mixture of **24** and $[Rh(L)(\eta^6\text{-}FC_6H_5)][BAr^F{}_4]$.

Scheme 7. Synthesis of Complex 24 by Direct and Indirect Routes[a]

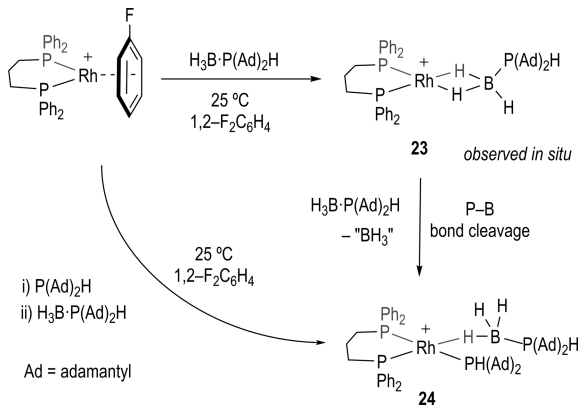

[a] $[BAr^F{}_4]^-$ anions are not shown.

The ^{1}H NMR spectrum of complex **23** immediately after preparation shows a broad, relative integral 3H, signal at δ −1.36 characteristic of a σ-bound phosphine−borane that is undergoing site exchange between the coordinated and uncoordinated B−H environments.[42] Two signals are observed in the ^{31}P{^{1}H} NMR spectrum, in a 2:1 ratio at δ 35.1 [J(RhP) 167 Hz] and δ 30.1 (br). Over time (1 h), complex **23** disappears to be replaced by a new complex that has been characterized by NMR spectroscopy and a solid-state X-ray diffraction experiment as $[Rh(L)(PHR_2)(\eta^1\text{−}H_3B{\cdot}PHR_2)][BAr^F{}_4]$ (**24**, R = adamantyl). Figure 4 shows the structure of the cation present in **24** in the solid-state. A Rh(I) center is in a pseudo-square-planar geometry with a chelating ligand, and the other two coordination sites are occupied by $P(adamantyl)_2H$ and a η^1-$H_3B{\cdot}P(adamantyl)_2H$ [Rh···B, 2.457(7) Å] ligands, respectively. The BH and PH hydrogen atoms were located in the final difference map. The solution NMR spectroscopic data for **24** are fully consistent with the solid-state structure, and in particular the *trans* disposition of P1 and P3, and the η^1-$H_3B{\cdot}PR_2H$ ligand.

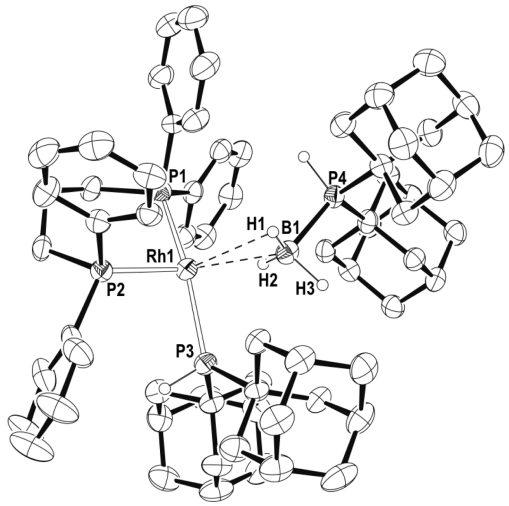

Figure 4. Molecular structure of the cation of **24**. Displacement ellipsoids are drawn at 50% probability level. Some hydrogen atoms are omitted for clarity. Selected bond lengths (Å): Rh1−P1, 2.2262(16); Rh1−P2, 2.2861(16); Rh1−P3, 2.3568(15); Rh1···B1, 2.457(7); B1−P4, 1.936(7).

A significant amount of P−B bond cleavage product is thus observed for both electron poor aryl phosphine−boranes (e.g., **14**) and very bulky electron rich phosphine−boranes (e.g., **24**), but *not* the electron rich aryl phosphine **3** or $H_3B{\cdot}PPh_2H$ (**6**).[31] Interestingly we have recently reported that for $H_3B{\cdot}P^tBu_2H$ P−B bond cleavage is also observed during dehydrocoupling catalysis being accompanied by a further dehydrocoupling step, through which bis(phosphine)boronium salts are ultimately formed.[30,36] Similar complexes can be prepared on rhodium using $H_3B{\cdot}PPh_2H$ and PPh_3 under stoichiometeric conditions.[36] One suggested mechanism for this process is the reaction of a short-lived phosphino−borane (or its masked equivalent) with coordinated phosphine, not dissimilar to the mechanism suggested for the formation of diaminoboranes from amine−boranes and amines catalyzed by alkaline earth catalysts.[55] Complexes **20** and **24** serve as models for intermediates in this process [Rh(III) and Rh(I), respectively], although we do not observe the formation of corresponding bis(phosphine)boronium salts in this case.

Stoichiometric Dehydrocoupling of Primary Phosphine−Boranes. The dehydrocoupling of primary phosphine−boranes can yield polyphosphinoboranes, rather than the simple oligomers observed with secondary phosphine−boranes (Scheme 1). With an appreciation of the intermediate metal complexes formed with secondary phosphine−boranes from this and previous work,[30,31,36] it was of interest to explore whether the proposed dehydrocoupling mechanism for secondary phosphine−boranes using $[Rh(L)(\eta^6\text{-}FC_6H_5)][BAr^F{}_4]$ could be applied to primary analogues. Such insight into the mechanism of dehydropolymerization of phosphine−boranes is important, as these processes currently remain unresolved due to the melt conditions employed that make following intermediates or kinetics problematic.[20,28,33]

In situ investigations using stoichiometric quantities of primary phosphine−boranes $H_3B{\cdot}PPhH_2$ resulted in immediate reaction when combined with $[Rh(L)(\eta^6\text{-}FC_6H_5)][BAr^F{}_4]$, but a number of products were formed which we have not been able to convincingly characterize. This mixture of species observed is in contrast with $H_3B{\cdot}PPh_2H$ where single products

dx.doi.org/10.1021/ic500032f | Inorg. Chem. 2014, 53, 3716−3729

are formed analogous to **14**–**16**.[31] However, reaction of $[Rh(L)(\eta^6\text{-}FC_6H_5)][BAr^F{}_4]$ with a slight excess of $H_3B{\cdot}PCyH_2$ (**5**) in 1,2-$F_2C_6H_4$ solution at 25 °C led to the instantaneous formation of only two complexes in a 1:1 ratio, **25a** and **25b**, $[Rh(L)H(\sigma,\eta\text{-}PCyH{\cdot}BH_3)(\eta^1\text{-}H_3B{\cdot}PCyH_2)][BAr^F{}_4]$, as a proposed diastereomeric pair (Scheme 8). This stereoisomerism

Scheme 8. Synthesis of 25a, 25b, and the Dehydrocoupled Products 26a and 26b[a]

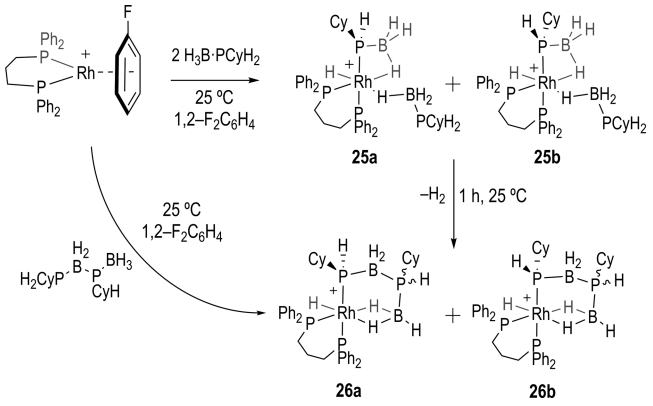

[a] $[BAr^F{}_4]^-$ anions are not shown.

comes from P–H activation at the prochiral primary phosphine. These new products are directly analogous to those formed with secondary phosphine–boranes (i.e., **14**), and the NMR spectroscopic data match closely. The $^{31}P\{^1H\}$ NMR spectrum from this reaction shows 8 resonances, in addition to a broad peak at δ −35.5 due to excess phosphine–borane, as each diastereomer contains four distinct phosphorus environments. Signals centered at δ 31.7 and 30.5 are assigned to one of the chelating phosphine ligand ^{31}P environments in each diastereoisomer, and show characteristic J(RhP) coupling constants consistent with a Rh(III) center. Complex overlapping multiplets at δ 11.8 [2 × ddd] represent the resonances for both diastereomers of the second chelated phosphorus center, which is *trans* to the phosphide position, displaying a large *trans* PP coupling constant [J(PP) ∼ 200 Hz] in addition to coupling to ^{103}Rh and *cis*-^{31}P. The remaining 4 signals are broad indicating the phosphorus centers are bound to a quadrupolar ^{11}B nucleus. Of these, peaks at δ −11.0 and −32.1 are assigned to the phosphide centers of each diastereomer *trans* to the chelating phosphine [J(PP) ∼200 Hz], and resonances at δ −39.8 and δ −44.2 as assigned to phosphorus centers in the σ-bound phosphine–borane unit. These large differences in chemical shift of the phosphido signal ($\Delta\delta$ 21.2) might reflect significant local difference in steric pressure between **25a** and **25b** at this group. Interestingly, a much smaller difference is observed with the dehydrocoupled products (**26a/b**, $\Delta\delta$ 3.5) in which the phosphide group is part of a chelate ring. The ^{1}H NMR spectrum does not have the necessary resolution to separate out the diastereomers in the hydride region, with broad resonances observed at δ −2.3 (3 H, BH_3), δ −7.9 (1 H, Rh–H–B), δ −17.5 (Rh–H).

Complexes **25a/b** cannot be isolated in pure form, and characterization by NMR spectroscopy is best performed on freshly prepared samples, as after 1 h (25 °C) they have undergone dehydrocoupling to give a mixture of two resolvable diastereomers **26a** and **26b**, with one of the diastereomers present in a significantly larger amount ∼6:1 (Scheme 8), indicating that the dehydrocoupling step occurs with some stereocontrol.[56] The decomposition product $[Rh(L)(PH_2Cy)_2]^+$, analogous to **21**/**22**, was also observed. NMR spectroscopic and ESI-MS analysis suggests that the dehydrocoupling products formed are direct analogues of **17**. This mixture of diastereomers can also be synthesized cleanly by direct reaction of $[Rh(L)(\eta^6\text{-}FC_6H_5)][BAr^F{}_4]$ with the preformed diaboraphosphine $H_3B{\cdot}PCyHBH_2{\cdot}PCyH_2$ (**13**) in 1,2-$F_2C_6H_4$ solution at 25 °C (Figure 5 for the solid-state

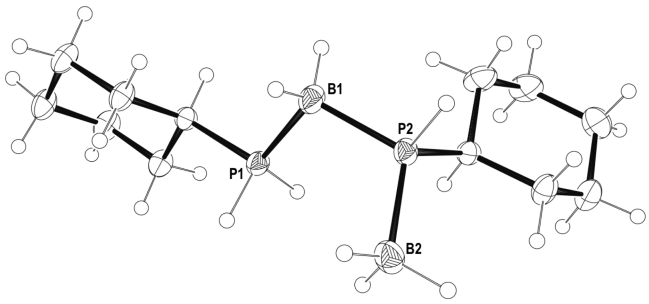

Figure 5. Molecular structure of **13**. Displacement ellipsoids are drawn at 50% probability level. Selected bond lengths (Å) and angles (deg): P1–B1 1.9267(18), B1–P2 1.9381(18), P2–B2 1.926(2); P1–B1–P2 108.34(9), B1–P2–B2 113.32(9).

structure). Immediate measurement of the $^{31}P\{^1H\}$ NMR spectrum after mixing showed clean conversion to complexes **26a** and **26b** in an approximate 1:1 ratio, interestingly different from the 1:6 ratio observed from dehydrocoupling.

Resonances in the $^{31}P\{^1H\}$ NMR spectrum of **26** can, again, be assigned aided by reference to those of structurally characterized **17**. Peaks centered at δ 37.9 and 34.5 result from the chelated phosphorus *trans* to the B-agostic site, while the signals for the phosphorus *trans* to the phosphido group overlap at δ 10.7, and display characteristic J(PP) *trans* coupling [255 Hz]. The broad resonances of the diboraphosphine are observed at δ 19.8 and 16.2 for the phosphido center [J(PP) 255] and δ −14.9 and −16.6 ppm for the remaining site. The high-field region of the ^{1}H NMR spectrum of **26a**/**26b** shows a slight downfield shift of the Rh–H hydride resonance to δ −16.1, when compared to **25a**/**25b**, while the η^2-BH_2···Rh units are observed as two broadened resonances at δ −2.98 (1H) and δ −5.98 (1H). For these hydride signals the separate signals are not resolved for each diasteroisomer, although each resonance is rather asymmetric suggesting two overlapping environments.

A $^{31}P\{^1H\}$ NMR spectrum taken of this mixture after 18 h at 25 °C showed a significant change in the ratios of the diastereomers **26a**/**26b** (Scheme 9). The peaks for one isomer at [δ 34.5, 16.2, 10.7, and −14.9] have reduced relative area, giving an approximate ratio of 6:1 for the two diastereoisomers. This ratio is similar to that found from direct dehydrocoupling in **25a**/**25b** after 1 h (*vide supra*), underscoring the stereocontrol occurring in the P–B bond forming process. Leaving this solution for one week resulted in no significant change to this ratio, suggesting equilibrium had been reached. We suggest that the mechanism for equilibration involves reductive elimination of the phosphido and hydride ligands to form a Rh(I) σ phosphine–borane complex,[30] similar to **E** in Scheme 2, which then undergoes rapid oxidative addition of the other P–H bond. This must be a reversible process, leading to a thermodynamic ratio of the diastereoisomers and the resulting

dx.doi.org/10.1021/ic500032f | Inorg. Chem. 2014, 53, 3716–3729

Scheme 9. Change in Diastereoisomeric Ratio and Release of the Diboraphosphine[a]

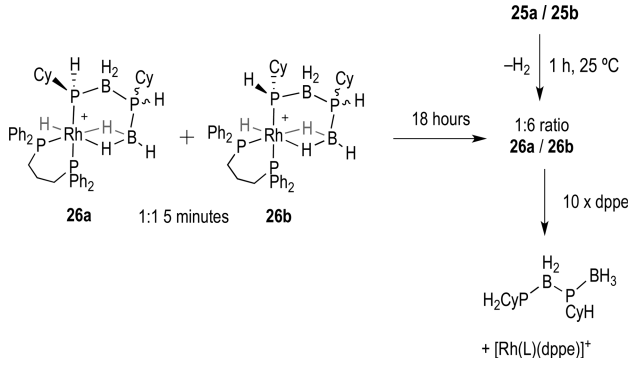

[a] $[BAr^F_4]^-$ anions are not shown.

selectivity. Unfortunately we were unable to deduce the stereochemistry of the preferred isomer using ROESY experiments or a solid-state structure. However, inspection of models leads us to propose that the thermodynamic product is likely to have the cyclohexyl group pointing away from the chelating phosphine ligand's phenyl groups, i.e., **26b**. That these diastereoisomers are a result of the metal activation of the prochiral terminal P–H bonds in **13** is shown by addition of an excess of dppe to **26a/b**.[56] This affords $[Rh(dppe)(L)][BAr^F_4]$[31] with the concomitant formation of free **13** (Scheme 9).

We have briefly explored the use of a chiral metal/ligand fragment in dehydrocoupling, $[Rh(BDPP)]^+$ [*S,S*-BDPP = (2*S*,4*S*)-2,4-bis(diphenylphosphino)pentane]. This chiral ligand was chosen as electronically and sterically (i.e., bite angle) it is similar to $Ph_2P(CH_2)_3PPh_2$. Addition of $H_3B{\cdot}PCyH_2$, **5**, to $[Rh(BDPP)(\eta^6\text{-}FC_6H_5)][BAr^F_4]$ results in the immediate formation of *two* diastereoisomers of $[Rh(BDPP)H(\sigma,\eta\text{-}PCyHBH_3)(\eta^1\text{-}H_3B{\cdot}PCyH_2)][BAr^F_4]$, **27**, in a 3:1 ratio (Scheme 10). Although we are unable to comment on the

Scheme 10. Use of a Chiral Ligand in Dehydrocoupling[a]

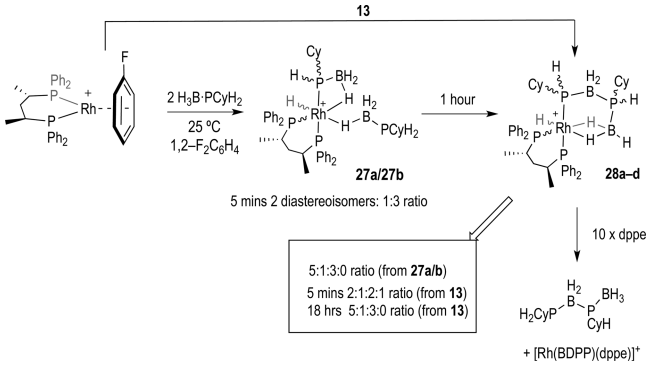

[a] $[BAr^F_4]^-$ anions are not shown.

absolute configuration of these isomers, it is interesting to note that this is biased away from the 1:1 ratio observed in the achiral system. Compounds **27a/b** proceed on to dehydrocouple to form diastereoisomers of $[Rh(BDPP)H(\sigma,\eta^2\text{-}PRH{\cdot}BH_2PRH{\cdot}BH_3)][BAr^F_4]$, **28**, 1:5:3:0 ratio. The same mixture of diasteroisomers can be formed by direct addition of **13** to $[Rh(BDPP)(\eta^6\text{-}FC_6H_5)][BAr^F_4]$. Initially a 2:1:2:1 ratio of 4 isomers is observed, that changes to a 5:1:3:0 ratio after 18 h. We are unable to comment in more detail on the conformation of these isomers, although the observation of stereocontrol in the direct dehydrocoupling is similar to that observed for the achiral system. Addition of excess dppe to this mixture forms a product identified by ESI-MS as $[Rh(BDPP)(dppe)]^+$ and free **13** (by ^{31}P and ^{11}B NMR spectroscopy). We have not explored whether there is enantiocontrol at the central {PCyH unit} arising from this PB coupling event on release from the metal.

For these experiments with $H_3B{\cdot}PCyH_2$ it is interesting to note that P–H activation is rapid and reversible with the Rh(I) precursor. This is in contrast to results obtained with secondary phosphine–boranes $H_3B{\cdot}P^tBu_2H$ and $H_3B{\cdot}P^tBu_2BH_2{\cdot}P^tBu_2H$, which on addition to $[Rh(L)(\eta^6\text{-}FC_6H_5)][BAr^F_4]$ gave the corresponding Rh(I) σ-phosphine–borane complexes with no P–H activation.[31] Such selectivity for primary over secondary phosphines in P–H activation at a metal center has been described previously for both phosphine[57] and phosphine–borane ligands.[27] In particular it has been shown that addition of $H_3B{\cdot}PPhH_2$ to $Pt(PEt_3)_2H(PPh_2{\cdot}BH_3)$ results in exchange of the metal bound phosphide complex to give the primary phosphido–borane complex.[26] Here it was suggested that the greater thermodynamic driving force for formation of the primary phosphido–borane complex comes from steric effects, as M–P bonds to smaller primary phosphido ligands are likely to be stronger.

Catalytic Dehydrocoupling of Secondary Phosphine–Boranes. Under the standard catalytic melt conditions (90 °C, 5 mol %),[20] $[Rh(L)(\eta^6\text{-}FC_6H_5)][BAr^F_4]$ will dehydrocouple the secondary aryl phosphine–boranes used in this study to form the corresponding linear diboraphosphines **10–12**, although we have not explored in detail the temporal evolution of these systems due to the problems associated with directly interrogating the melt. However, trends can be observed. For electron-withdrawing groups (**1** and **2**), complete consumption of starting material occurs in 4 h (Table 1). The reaction at this

Table 1. Conversion of $H_3B{\cdot}PR_2H$ with Time[a]

$H_3B{\cdot}PR_2H$	time/h	$H_3B{\cdot}PR_2H$/%	$H_3B{\cdot}PR_2BH_2PR_2H$/%	$(BH_2PR_2)_n$/%
1	1	10	55	<5
	4	<5	45	10
	8	<5	35	50
2	1	10	70	10
	4	<5	70	15
	8	<5	70	15
3	1	50	30	<5
	4	30	45	5
	8	20	60	5

[a] R = aryl, see Figure 1. [Cat.] = $[Rh(L)(\eta^6\text{-}FC_6H_5)][BAr^F_4]$, L = $Ph_2P(CH_2)_3PPh_2$. Conversions calculated from $^{31}P\{^1H\}$ NMR spectra. Conditions: $[Rh(L)(\eta^6\text{-}FC_6H_5)][BAr^F_4]$, 5 mol %, 90°C, melt.

temperature is not selective, and although the main product is the linear diboraphosphine, there are products that we tentatively identify as the cyclic oligomers $(BH_2PR_2)_n$ (n = 3, 4).[20,33] Our results are broadly in line with the previously reported catalyzed dehydrocoupling of **2** using $[Rh(COD)Cl]_2$, which, at a slightly lower temperature (60 °C, 16 h, melt), affords the linear diboraphosphine product in 69% isolated yield, while at 100 °C only the cyclic oligomers are isolated. The mechanism of formation of the higher cyclic oligomers, $(BH_2PR_2)_n$, remains to be resolved.[20] For electron-donating **3** the reaction is slower using the $[Rh(L)(\eta^6\text{-}FC_6H_5)][BAr^F_4]$

dx.doi.org/10.1021/ic500032f | Inorg. Chem. 2014, 53, 3716–3729

catalyst (8 h) but overall is more selective. For R = Ph we have previously shown that $[Rh(L)(\eta^6\text{-}FC_6H_5)][BAr^F{}_4]$ catalyzes dehydrocoupling to give the corresponding linear diboraphosphine in greater than 95% conversion after 4 h.[31] For secondary phosphine–boranes, $H_3B{\cdot}PPh_2H$ thus offers balance between overall rate and selectivity.

Given the product distributions and likely decomposition pathways in the melt it is inappropriate to comment in detail on the nature of the rate-determining steps during catalysis under these conditions. However, on the basis of the solution studies, P–B bond formation, (dehydrocoupling) is faster with electron-withdrawing groups. The temporal differences in observed product conversion in the melt could reflect a difference in the rate of the P–B bond forming event, or alternatively, they could reflect the ease at which the bound product is substituted on the metal center, i.e., a turnover limiting step. To probe this latter scenario, reaction between **19** (aryl-OMe) and diboraphosphine **11** (aryl-CF_3) to form **18** and free **12** demonstrates that an equilibrium is established slightly in favor of **18** (Scheme 11). This suggests that there is not a

Scheme 11. Competition Experiments between Linear Diboraphosphines[a]

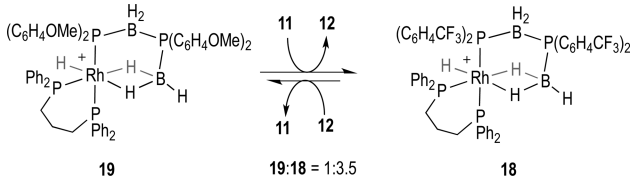

[a] $[BAr^F{}_4]^-$ anions are not shown.

strong inherent difference in binding strengths between the two products, with the implication being that the observed rate differences *in the melt* arise from the dehydrocoupling step. Although this is different from what is observed in solution at room temperature, in which release of the product is likely the turnover limiting step, it is consistent with the high local concentration of $H_3B{\cdot}PR_2H$ that being under melt conditions (90 °C) would promote such a substitution.

Catalytic Dehydrocoupling of Primary Phosphine–Boranes. $[Rh(L)(\eta^6\text{-}FC_6H_5)][BAr^F{}_4]$ also acts as a catalyst for the dehydrocoupling of primary phosphine–boranes. Under melt conditions (90 °C, 5 mol %, 4 h) $H_3B{\cdot}PPhH_2$ is dehydrocoupled to give a major product which is identified by ^{31}P NMR spectroscopy as being polymeric $(BH_2PPhH)_n$ by comparison with previously reported[19,20] data for purified material coming from the $[Rh(COD)_2][OTf]$ catalyzed process [δ −49.3, d, J(PH) ∼350 Hz, 1,2-$F_2C_6H_4$; lit.: δ −48.9, δ, J(PH) 360 Hz, $CDCl_3$]. There were also other species observed ∼δ −55, which could be reduced in relative concentration (to ∼10%) by precipitation into hexanes. Such species have been previously suggested to be short-chain oligomers.[20] Interestingly, these proposed shorter chain oligomers are present in a greater proportion at shorter reaction times, which might suggest that polycondensation is occurring to give higher molecular weight polymer. Under non-melt conditions[20] (toluene heated to reflux, 0.5 mol %, 16 h) these shorter oligomers are by far the dominant species (Supporting Information). It thus appears that a high local concentration of phosphine–borane is necessary for productive dehydropolymerization. Positive mode ESI-MS (electrospray mass spectrometry) of the melt reaction product demonstrated polymerization, showing repeat units of $[H\text{-}(PPhHBH_2)_nPPhH_2]^+$ up to n = 10 (Supporting Information). Similar analyses have been reported for amine–borane dehydropolymerization.[12,14,58] That these polymers are terminated by $\{PPhH_2\}$ groups rather than $\{BH_3\}$ is confirmed by inspection of the corresponding isotopomer patterns. This formulation also argues against cyclic oligomers being observed by ESI-MS, and presumably the additional phosphine arises from P–B bond cleavage. Use of $H_3B{\cdot}PCyH_2$ under these conditions afforded significantly more complex mixtures that we were unable to resolve.

CONCLUSIONS

The solid-state structures of the intermediates in the dehydrocoupling of secondary phosphine–boranes using the $\{Rh(Ph_2PCH_2CH_2CH_2PPh_2)\}^+$ fragment have been determined. This demonstrates that the complex that precedes dehydrocoupling to form a linear diboraphosphine has σ bound and P–H activated phosphine–borane ligands, while the product has a linear diboraphosphine bound to the metal center. For aryl phosphine–boranes, electron-withdrawing groups (CF_3) promote stoichiometric dehydrocoupling faster than for more electron-donating (OMe) groups. This increase in rate is accompanied by a significant degree of parallel and competitive P–B bond cleavage to afford metal complexes with two monodentate phosphine ligands, which we suggest is due to a weakening of the P–B bond with electron-withdrawing aryl groups. These systems also turnover catalytically under melt conditions, with the overall rate of conversion broadly following the relative dehydrocoupling rates observed in the stoichiometric studies, suggesting that the dehydrocoupling step under melt conditions might also be the turnover limiting step. P–B bond cleavage also occurs for very bulky electron rich adamantyl phosphine–boranes, to such an extent that stoichiometric dehydrocoupling is not observed. For this phosphine–borane we suggest that sterics play a role in this process.

A significant observation is that, for primary phosphine–boranes, which are precursors to polyphosphinoboranes, use of the $\{Rh(Ph_2PCH_2CH_2CH_2PPh_2)\}^+$ fragment results in some apparent diastereoselectivity in the dehydrocoupling step, at least in the stoichiometric reactions that produce metal-bound diboraphosphines. Such selectivity could well have implications in the control of the stereochemistry of polymer that would result from further insertion events. A significant future challenge is to harness any inherent bias in each dehydrocoupling insertion step productively while also developing the necessary spectroscopic and physical characterization markers to interrogate the oligomer and polymer stereochemistry.

EXPERIMENTAL SECTION

All manipulations, unless otherwise stated, were performed under an atmosphere of argon, using standard Schlenk and glovebox techniques. Glassware was oven-dried at 130 °C overnight and flamed under vacuum prior to use. Hexane and pentane were dried using a Grubbs type solvent purification system (MBraun SPS-800) and degassed by successive freeze–pump–thaw cycles.[59] CD_2Cl_2, C_6H_5F, and 1,2-$F_2C_6H_4$ were distilled under vacuum from CaH_2 and stored over 3 Å molecular sieves, 1,2-$F_2C_6H_4$ was stirred over alumina for 2 h prior to drying. Bis-1,3-(diphenylphosphino)propane (dpp3) and (2*S*,4*S*)-2,4-bis(diphenylphosphino)pentane (BDPP) were purchased from Aldrich. $[Rh(nbd)Cl]_2$[60] and $[Rh(nbd)(dpp3)][BAr^F{}_4]$[16] were prepared as previously described. (4-Methoxyphenyl)$_2$HP·BH_3 (**3**),

dx.doi.org/10.1021/ic500032f | Inorg. Chem. 2014, 53, 3716–3729

(adamantyl)$_2$HP·BH$_3$ (**4**), and CyH$_2$P·BH$_3$ (**5**) were prepared by the same method as Me$_3$P·BH$_3$[61] but with the phosphine changed. (4-Trifluoromethylphenyl)$_2$PH·BH$_3$ (**2**) and (3,5-bis(trifluoromethyl)-phenyl)$_2$PCl were prepared according to literature procedures reported by Clark et al.[33] NMR spectra were recorded on a Bruker AVD 500 MHz spectrometer at room temperature unless otherwise stated. In 1,2-C$_6$H$_4$F$_2$, ^{1}H NMR spectra were referenced to the center of the downfield solvent multiplet (δ 7.07), and ^{31}P and ^{11}B NMR spectra were referenced against 85% H$_3$PO$_4$ (external) and BF$_3$·OEt$_2$ (external), respectively. The spectrometer was prelocked and preshimmed using a C$_6$D$_6$ (0.1 mL) and 1,2-C$_6$H$_4$F$_2$ (0.3 mL) sample. Chemical shifts are quoted in ppm and coupling constants in Hz. ESI-MS were recorded on a Bruker micrOTOF instrument.[62] In all ESI-MS spectra there was a good fit to both the principal molecular ion and the overall isotopic distribution. Signals in the ^{31}P{^{1}H} NMR spectra were integrated relative to those in similar environments (i.e., Rh−P or B−P) to obtain the relative ratios of products, and data was acquired with a pulse repetition time of 1 s. This avoids potential problems with different relaxation times for different phosphorus environments. Nevertheless, the quoted relative ratios based upon this data should be treated as qualitative rather than quantitative.

Synthesis and Characterization of New Complexes. *Synthesis of H$_3$B·PR$_2$H [R = 3,5-Bis(trifluoromethyl)phenyl] (**1**).* A solution of (3,5-bis(trifluoromethyl)phenyl)$_2$PCl (1.48 g, 3.0 mmol) in diethyl ether (5 mL) was added dropwise to a diethyl ether (20 mL) suspension of LiBH$_4$ (0.070 g, 3.21 mmol) cooled to 5 °C with an ice bath. The mixture became cloudy immediately and was allowed to stir for 30 min. The diethyl ether was removed *in vacuo*, and the residue was dissolved in hexanes (30 mL) and filtered through Celite. The hexanes were reduced *in vacuo* to ∼10 mL, and the solution was placed in the freezer (−20 °C) overnight yielding colorless crystals. Excess hexanes were decanted, and crystals were dried to afford a fine white powder which was subsequently washed with 2 × 3 mL of cold hexanes. Removal of all volatiles under reduced pressure yielded 630 mg of fine white powder (**1**).

^{1}H NMR (300 MHz, CDCl$_3$): δ 8.14 (br s, 1 H, *p*-Ar-H), 8.09 (br s, 2 H, *o*-Ar-H), 6.58 (dm, $^1J_{HP}$ = 388 Hz, 1 H, PH), 0.3−2.0 (br m, 3 H, BH). ^{31}P{^{1}H} NMR (121 MHz, CDCl$_3$): δ 4.7 (br s, PH). ^{11}B{^{1}H} NMR (160 MHz, CDCl$_3$): δ −41.7 (br s, BH$_3$). ^{19}F NMR (282 MHz, CDCl$_3$): δ −62.9 (s, CF$_3$). EI-MS (70 eV) *m*/*z* (%): 458 (62) [M$^+$ − BH$_3$]. Anal. Found: C 40.71%, H 2.02%. Calcd for C$_{16}$H$_{10}$BF$_{12}$P: C 40.68%, H 2.14%.

*Synthesis of (Adamantyl)$_2$PH·BH$_3$ (**4**).* (Adamantyl)$_2$PH·BH$_3$ was prepared under the same conditions as Me$_3$P·BH$_3$[61] but with (adamantyl)$_2$PH instead of PMe$_3$.

^{1}H NMR (300 MHz, CDCl$_3$): δ 3.61 (dm, 1 H, $^1J_{HP}$ = 379 Hz, PH), 2.11 to 1.83 (30 H, adamantyl-H), 0.41 to −0.15 (br m, 3 H, BH). ^{31}P{^{1}H} NMR (121 MHz, CDCl$_3$): δ 40.1 (br m, PH). ^{11}B{^{1}H} NMR (160 MHz, CDCl$_3$): δ −44.8 (br d, BH$_3$). Anal. Found: C 75.78%, H 10.71%. Calcd for C$_{20}$H$_{34}$BP: C 75.89%, H 10.84%.

*Synthesis of H$_3$B·PR$_2$BH$_2$·PR$_2$H [R = 3,5-Bis(trifluoromethyl)phenyl (**10**); 4-Trifluoromethylphenyl (**11**); 4-Methoxyphenyl (**12**)].* A Youngs flask charged with 0.25 mmol of R$_2$PH·BH$_3$ (118 mg of **1**, 84 mg of **2**, 65 mg of **3**) and 5 mol % of [Rh(dpp3)(C$_6$H$_5$F)][BAr$^F_4$] (18.4 mg, 0.0125 mmol) was heated to 90 °C for 4 h (**10** and **11**) or 8 h (**12**) in melt conditions. The resulting solids were washed with *n*-hexane and recrystallized from a mixture of diethyl ether and hexane at −18 °C (**10** 30 mg, 25%; **11** 22 mg, 26%; **12** 32 mg, 49%).

Details follow for **10**. ^{1}H NMR (300 MHz, CDCl$_3$): δ 8.09 to 7.89 (12 H, Ar−H), 7.32 (dm, $^1J_{HP}$ = 412 Hz, 1 H, PH), 2.45 (br m, 2 H, BH$_2$), 1.11 (br m, 3 H, BH$_3$). ^{31}P{^{1}H} NMR (121 MHz, CDCl$_3$): δ −1.7 (br s, PHR$_2$), −14.0 (br s, PR$_2$). ^{11}B{^{1}H} NMR (160 MHz, CDCl$_3$): δ −33.2 (br s, BH$_2$), −37.7 (br s, BH$_3$). Anal. Found: C 40.90%, H 1.83%. Calcd for C$_{32}$H$_{18}$B$_2$F$_{24}$P$_2$: C 40.76%, H 1.93%.

Details follow for **11**. ^{1}H NMR (500 MHz, CD$_2$Cl$_2$): δ 7.77 to 7.52 (16 H, Ar−H), 7.04 (dt, $^1J_{HP}$ = 426 Hz, $^3J_{HH}$ = 7.8 Hz, 1 H, PH), 2.37 (br m, 2 H, BH$_2$), 1.02 (br m, 3 H, BH$_3$). ^{31}P{^{1}H} NMR (202 MHz, CD$_2$Cl$_2$): δ −3.5 (br s, PHR$_2$), −15.4 (br s, PR$_2$). ^{11}B{^{1}H} NMR (160 MHz, CD$_2$Cl$_2$): δ −33.7 (br s, BH$_2$), −37.6 (br s, BH$_3$).

Details follow for **12**. ^{1}H NMR (500 MHz, CD$_2$Cl$_2$): δ 7.64 to 6.77 (16 H, Ar−H), 6.69 (dt, $^1J_{HP}$ = 415 Hz, $^3J_{HH}$ = 6.6 Hz, 1 H, PH), 3.84 (s, 6 H, CH$_3$), 3.80 (s, 6 H, CH$_3$), 2.14 (br m, 2 H, BH$_2$), 0.96 (br m, 3 H, BH$_3$). ^{31}P{^{1}H} NMR (202 MHz, CD$_2$Cl$_2$): δ −7.6 (br s, PHR$_2$), −22.1 (br s, PR$_2$). ^{11}B{^{1}H} NMR (160 MHz, CD$_2$Cl$_2$): δ −33.3 (br s, BH$_2$), −37.1 (br s, BH$_3$).

*Synthesis of [Rh(dpp3)H(PR$_2$·BH$_3$)(H$_3$B·PHR$_2$)][BAr$^F_4$] [R = 3,5-Bis(trifluoromethyl)phenyl (**14**); 4-Trifluoromethylphenyl (**15**); 4-Methoxyphenyl (**16**)].* To a Youngs flask charged with [Rh(dpp3)-(C$_6$H$_5$F)][BAr$^F_4$] (50 mg, 0.034 mmol) and 2 equiv of H$_3$B·PR$_2$H (32 mg of **1**, 23 mg of **2**, 18 mg of **3** 0.068 mmol) was added 1,2-F$_2$C$_6$H$_4$ (5 mL). The solution was stirred at room temperature 10 min, and a change in color from pale orange to bright yellow was observed. Complexes **15** and **16** were isolated as yellow oils, and characterized *in situ* by NMR spectroscopy and ESI-MS. Complex **14** could be crystallized at −24 °C in the freezer inside the glovebox (yield 29.6 mg, 37%). Complexes **15** and **16** could not be isolated cleanly, and attempts to do so led to intractable mixtures of **15** and **16** with **18** and **19**, respectively.

Details follow for **14**. Slow diffusion of pentane (10 mL) over a solution of **14** in 1,2-F$_2$C$_6$H$_4$ at −24 °C afforded yellow crystals (one of which was employed for an X-ray diffraction study).

^{1}H NMR (500 MHz, 1,2-F$_2$C$_6$H$_4$): δ 8.32 (s, 8 H, BAr$^F_4$), 7.69 (s, 4 H, BAr$^F_4$), 5.81 (d, $^1J_{HP}$ = 435 Hz, 1 H, PH), 3.12−0.81 (8 H, 3CH$_2$ dpp3 + BH$_2$), −0.78 (br, 3 H, BH$_3$), −6.12 (br, 1 H, BH−Rh), −16.21 (s, 1 H, Rh−H). Signals from the aromatics were not observed due to being overlapped by signals from 1,2-F$_2$C$_6$H$_4$.

^{1}H NMR (500 MHz, 1,2-F$_2$C$_6$H$_4$, selected data at 0 °C): δ −6.12 (d, $^1J_{HP}$ = 65 Hz, 1 H, BH−Rh). ^{31}P{^{1}H} NMR (202 MHz, 1,2-F$_2$C$_6$H$_4$): δ 29.5 (ddd, J_{PRh} = 130 Hz, $J_{PP(cis)}$= 35 Hz, $J_{PP(cis)}$ = 21 Hz, Ph$_2$P(CH$_2$)$_3$PPh$_2$), 11.3 (ddd, $J_{PP(trans)}$ = 244 Hz, J_{PRh} = 103 Hz, $J_{PP(cis)}$ = 35 Hz, Ph$_2$P(CH$_2$)$_3$PPh$_2$), −0.7 (dd, $J_{PP(trans)}$ = 248 Hz, J_{PRh} = 75 Hz, Rh-PR$_2$BH$_3$), −2.62 (br s, PHR$_2$BH$_3$). ^{11}B{^{1}H} NMR (160 MHz, 1,2-F$_2$C$_6$H$_4$): δ −6.2 (BAr$^F_4$), −39.8 (br, 2 × BH$_3$). ESI-MS (1,2-C$_6$H$_4$F$_2$, 60 °C) positive ion: *m*/*z* = 1431.07 (calcd 1431.07, M$^+$ − 2BH$_3$). Anal. Found: C 46.82%, H 2.39%. Calcd for C$_{91}$H$_{58}$B$_3$F$_{48}$P$_4$Rh: C 47.02%, H 2.52%.

Details follow for **15**. ^{1}H NMR (500 MHz, 1,2-F$_2$C$_6$H$_4$): δ 8.32 (s, 8 H, BAr$^F_4$), 7.69 (s, 4 H, BAr$^F_4$), 4.90 (d, J_{HP} = 414 Hz, PH), 3.01−1.10 (8 H, 3CH$_2$ dpp3 + BH$_2$), −1.18 (br, 3H, BH$_3$), −6.95 (d, J_{HP} = 78 Hz, 1 H, BH−Rh), −16.51 (s, 1 H, Rh−H). Signals from the aromatics were not observed due to being overlapped by signals from 1,2-F$_2$C$_6$H$_4$. ^{31}P{^{1}H} NMR (202 MHz, 1,2-F$_2$C$_6$H$_4$): δ 27.3 (ddd, J_{PRh} = 127 Hz, $J_{PP(cis)}$ = 37 Hz, $J_{PP(cis)}$ = 16 Hz, Ph$_2$P(CH$_2$)$_3$PPh$_2$), 11.8 (ddd, $J_{PP(trans)}$ = 231 Hz, J_{PRh} = 100 Hz, $J_{PP(cis)}$ = 37 Hz, Ph$_2$P(CH$_2$)$_3$PPh$_2$), −0.3 (dd, $J_{PP(trans)}$ = 231 Hz, J_{PRh} = 70 Hz, Rh-PR$_2$BH$_3$), −5.96 (br s, PHR$_2$BH$_3$). ^{11}B{^{1}H} NMR (160 MHz, 1,2-F$_2$C$_6$H$_4$): δ −6.2 (BAr$^F_4$) −39.9 (br, 2 × BH$_3$). ESI-MS (1,2-C$_6$H$_4$F$_2$, 60 °C) positive ion: *m*/*z* = 1159.13 (calcd 1159.13, M$^+$ − 2BH$_3$).

Details follow for **16**. ^{1}H NMR (500 MHz, 1,2-F$_2$C$_6$H$_4$): δ 8.32 (s, 8 H, BAr$^F_4$), 7.69 (s, 4 H, BAr$^F_4$), 4.93 (d, J_{HP} = 409 Hz, 1 H, PH), 3.77 (s, 6 H, −OCH$_3$), 3.69 (s, 6 H, −OCH$_3$), 3.16−0.58 (8 H, 3CH$_2$ dpp3 + BH$_2$), −1.11 (br, 3 H, BH$_3$), −6.53 (d, J_{HP} = 73 Hz, 1 H, BH−Rh), −16.49 (s, 1 H, Rh−H). Signals from the aromatics were not observed due to being overlapped by signals from 1,2-F$_2$C$_6$H$_4$. ^{31}P{^{1}H} NMR (202 MHz, 1,2-F$_2$C$_6$H$_4$): δ 27.3 (ddd, J_{PRh} = 132 Hz, $J_{PP(cis)}$ = 37 Hz, $J_{PP(cis)}$ = 12 Hz, Ph$_2$P(CH$_2$)$_3$PPh$_2$), 9.5 (ddd, $J_{PP(trans)}$ = 227 Hz, J_{PRh} = 98 Hz, $J_{PP(cis)}$ = 37 Hz, Ph$_2$P(CH$_2$)$_3$PPh$_2$), 0.7 (br dd, $J_{PP(trans)}$ = 227 Hz, J_{PRh} = 65 Hz, Rh-PR$_2$BH$_3$), −11.2 (br s, PHR$_2$BH$_3$). ^{11}B{^{1}H} NMR (160 MHz, 1,2-F$_2$C$_6$H$_4$): δ −6.2 (BAr$^F_4$) −38.7 to −49.8 (br, 2 × BH$_3$). ESI-MS (1,2-F$_2$C$_6$H$_4$, 60 °C) positive ion: *m*/*z* = 1021.25 (calcd 1021.25, M$^+$ − BH$_3$), 914.19 (calcd 914.20, M$^+$ − BH$_3$ − C$_6$H$_4$OMe), 900.17 (calcd 900.17, M$^+$ − 2BH$_3$, −C$_6$H$_4$OMe), 775.17 (calcd 775.17, M$^+$ − (MeOC$_6$H$_4$)$_2$HP·BH$_3$).

*Synthesis of [Rh(dpp3)H(PR$_2$·BH$_2$PR$_2$·BH$_3$)][BAr$^F_4$] [R = 3,5-Bis-(trifluoromethyl)phenyl (**17**); 4-Trifluoromethylphenyl (**18**); 4-Methoxyphenyl (**19**)].* Method A follows. To a Youngs flask charged with [Rh(dpp3)(C$_6$H$_5$F)][BAr$^F_4$] (50 mg, 0.034 mmol) and 2 equiv of H$_3$B·PR$_2$H (32 mg of **1**, 23 mg of **2**, 18 mg of **3** 0.068 mmol) was added 1,2-F$_2$C$_6$H$_4$ (5 mL). The solution was stirred at room

dx.doi.org/10.1021/ic500032f | Inorg. Chem. 2014, 53, 3716−3729

temperature for 24 h. The formation of H_2 gas is also observed. Complex **19** was isolated as yellow oil (37 mg, 61%). Complexes **17** and **18** could not be isolated cleanly; they were observed with **22** and **23**, respectively.

Method B follows. To a Youngs flask charged with [Rh(dpp3)-(C_6H_5F)][BAr^F_4] (50 mg, 0.034 mmol) and 1 equiv of **10** (32 mg, 0.068 mmol) was added 1,2-$F_2C_6H_4$ (4 mL). Complex **17** was isolated as yellow solid (65 mg, 82%).

Details follow for **17**. Slow diffusion of pentane (10 mL) over a solution of **17** in 1,2-$F_2C_6H_4$ at −24 °C afforded yellow crystals (one of which was employed for an X-ray diffraction study).

^{1}H NMR (500 MHz, 1,2-$F_2C_6H_4$): δ 8.32 (s, 8H, BAr^F_4), 7.69 (s, 4H, BAr^F_4), 4.40 (vbr, 1H, BH) 3.10−2.12 (8H, 3CH_2 dpp3 + BH_2), −1.20 (vbr, 1H, B*H*), −4.54 (vbr, 1H, BH), −13.98 (s, 1H, Rh−H). Signals from aromatics not observed due to being overlapped by signals from 1,2-$F_2C_6H_4$. $^{31}P\{^1H\}$ NMR (202 MHz, 1,2-$F_2C_6H_4$): δ 46.6 (dd, J_{Rh-P}= 111, $J_{P^2-P^1(cis)}$= 36, $Ph_2P(CH_2)_3PPh_2$), 29.5 (m, $J_{P-P(trans)}$ = 260, Rh-*P*$R_2BH_3PR_2HBH_3$), 12.8 (ddd, $J_{P-P(trans)}$ = 260, J_{Rh-P}= 91, $J_{P-P(cis)}$ = 33, $Ph_2P(CH_2)_3PPh_2$), −2.7 (s, Rh-PR_2BH_3*P*R_2HBH_3). $^{11}B\{^1H\}$ NMR (160 MHz, 1,2-$F_2C_6H_4$): δ 0.21 (br), −6.2 (s, BAr^F_4), −27.1 (br). ESI-MS (1,2-$F_2C_6H_4$, 60 °C) positive ion: *m*/*z* = 1457.09 (calcd 1457.12, M^+). Anal. Found: C 47.15%, H 2.34%. Calcd for $C_{91}H_{56}B_3F_{48}P_4Rh$: C 47.07%, H 2.43%.

Details follow for **18**. ^{1}H NMR (500 MHz, 1,2-$F_2C_6H_4$): δ 8.32 (s, 8 H, BAr^F_4), 7.69 (s, 4 H, BAr^F_4), 4.24 (v br, 1 H, BH), 2.61−1.72 (8 H, 3CH_2 dpp3 + BH_2), −1.29 (v br, 1 H, BH), −4.65 (v br, 1 H, BH), −14.90 (s, 1 H, Rh−H). Signals from aromatics not observed due to being overlapped by signals from 1,2-$F_2C_6H_4$. $^{31}P\{^1H\}$ NMR (202 MHz, 1,2-$F_2C_6H_4$): δ 42.5 (dd, J_{PRh} = 106 Hz, $J_{PP(cis)}$ = 34 Hz, $Ph_2P(CH_2)_3PPh_2$), 28.6 (m, $J_{PP(trans)}$ = 272 Hz, Rh-*P*$R_2BH_3PR_2HBH_3$), 15.3 (ddd, $J_{PP(trans)}$ = 272 Hz, J_{PRh} = 101 Hz, $J_{PP(cis)}$ = 33 Hz, $Ph_2P(CH_2)_3PPh_2$), −6.4 (s, Rh-$PR_2BH_3PR_2HBH_3$). $^{11}B\{^1H\}$ NMR (160 MHz, 1,2-$F_2C_6H_4$): δ 0.4 (br), −6.2 (s, BAr^F_4), −25.9 (br). ESI-MS (1,2-$F_2C_6H_4$) positive ion: *m*/*z* = 1185.17 (calcd 1185.18, M^+).

Details follow for **19**. ^{1}H NMR (500 MHz, 1,2-$F_2C_6H_4$): δ 8.32 (s, 8 H, BAr^F_4), 7.69 (s, 4 H, BAr^F_4), 3.77 (s, 3 H, −OCH_3), 3.76 (s, 3 H, −OCH_3), 3.69 (s, 6 H, −OCH_3), 2.85−1.72 (8 H, 3CH_2 dpp3 + BH_2), −1.03 (v br, 1 H, BH), −4.00 (v br, 1 H, BH), −14.55 (s, 1 H, Rh−H). Signals from aromatics not observed due to being overlapped by signals from 1,2-$F_2C_6H_4$. $^{31}P\{^1H\}$ NMR (202 MHz, 1,2-$F_2C_6H_4$): δ 42.7 (ddd, J_{PRh} = 109 Hz, $J_{PP(cis)}$ = 35 Hz, $J_{PP(cis)}$ = 12 Hz $Ph_2P(CH_2)_3PPh_2$), 28.1 (br m, $J_{PP(trans)}$ = 279 Hz, Rh-*P*$R_2BH_3PR_2HBH_3$), 12.5 (ddd, $J_{PP(trans)}$ = 279 Hz, J_{PRh} = 88 Hz, $J_{PP(cis)}$ = 12 Hz, $Ph_2P(CH_2)_3PPh_2$), −11.7 (br s, Rh-$PR_2BH_3PR_2HBH_3$). $^{11}B\{^1H\}$ NMR (160 MHz, $C_6H_4F_2$): δ 3.42 (br), −6.2 (s, BAr^F_4), −27.7 (br). ESI-MS (1,2-$F_2C_6H_4$) positive ion: *m*/*z* = 1033.27 (calcd 1033.27, M^+).

*Synthesis of [Rh(dpp3)(PHR_2)$_2$][BAr^F_4] [R = 3,5-Bis-(trifluoromethylphenyl) (**21**)].* Method A follows. To a Youngs flask charged with [Rh(dpp3)(C_6H_5F)][BAr^F_4] (50 mg, 0.034 mmol) and 2 equiv of $H_3B{\cdot}PR_2H$ (32 mg of **1**) was added 1,2-$F_2C_6H_4$ (5 mL). The solution was stirred at room temperature for 24 h. The formation of H_2 (gas) is also observed. Complex **21** could not be isolated cleanly as **17** was also observed.

Method B follows. To a Youngs flask charged with [Rh(dpp3)-(C_6H_5F)][BAr^F_4] (20 mg, 0.034 mmol) and 2 equiv of PHR_2 (31 mg, 0.068 mmol, R = 3,5-bis(trifluoromethyl)phenyl) was added 1,2-$F_2C_6H_4$ (1 mL). After stirring for 10 min the solution was evaporated to dryness and the solid washed with pentane (2 mL). Complex **21** was isolated as yellow solid (yield 17.8 mg, 57%).

^{1}H NMR (500 MHz, 1,2-$F_2C_6H_4$): δ 8.33 (s, 8 H, BAr^F_4), 7.69 (s, 4 H, BAr^F_4), 6.41 (dm, J_{HP} = 375 Hz, 2 H, PH), 2.62 (br, 4 H, 2 CH_2 dpp3), 2.17 (m, 2 H CH_2, dpp3). Signals from aromatics not observed due to being overlapped by signals from 1,2-$F_2C_6H_4$. $^{31}P\{^1H\}$ NMR (202 MHz, 1,2-$F_2C_6H_4$): δ 9.6 (m, 2P, AA′BB′M), 5.5 (m, 2P, AA′BB′M). ESI-MS (1,2-$F_2C_6H_4$) positive ion: *m*/*z* = 1431.04 (calcd 1431.07, M^+). Anal. Found: C 47.71%, H 2.21%. Calcd for $C_{91}H_{52}BF_{48}P_4Rh$: C 47.60%, H 2.28%.

*[Rh(dpp3)(PHR_2)$_2$][BAr^F_4] [R = 4-Trifluoromethylphenyl (**22**)].* Complex **22** was characterized by *in situ* NMR spectroscopy. ^{1}H NMR (500 MHz, 1,2-$F_2C_6H_4$): δ 8.33 (s, 8 H, BAr^F_4), 7.69 (s, 4 H, BAr^F_4), 5.91 (dm, J_{HP} = 359 Hz, 2 H, PH), 2.57 (br, 4 H, 2 × CH_2 dpp3), 2.06 (m, 2 H × CH_2, dpp3). Signals from aromatics not observed due to being overlapped by signals from 1,2-$F_2C_6H_4$. $^{31}P\{^1H\}$ NMR (202 MHz, 1,2-$F_2C_6H_4$): δ 12.2 (m, 2P, AA′BB′M), 5.2 (m, 2P, AA′BB′M).

*Synthesis of [Rh(dpp3)(η^2-$H_3B{\cdot}PR_2H$)][BAr^F_4] [R = Adamantyl (**23**)].* To a Youngs flask charged with [Rh(dpp3)(C_6H_5F)][BAr^F_4] (50 mg, 0.034 mmol) and $H_3B{\cdot}PR_2H$ (**4**) (11 mg, 0.034 mmol) was added 1,2-$F_2C_6H_4$ (5 mL). The solution was stirred at room temperature for 1 min, and a change in color from pale orange to purple was observed. Complex **23** could not be isolated because further reaction to form **24** occurred.

^{1}H NMR (500 MHz, 1,2-$F_2C_6H_4$): δ 8.32 (s, 8 H, BAr^F_4), 7.68 (s, 4 H, BAr^F_4), 3.45 (d, 1 H, $^1J_{HP}$ = 380 Hz, B-PH), 2.52−1.12 (36 H, adamantyl-H + dpp3 CH_2), −1.36 (br, 3 H, BH_3). Signals from aromatics not observed due to being overlapped by signals from 1,2-$F_2C_6H_4$. $^{31}P\{^1H\}$ NMR (202 MHz, 1,2-$F_2C_6H_4$): δ 35.1 (d, J_{PRh} = 167 Hz, dpp3), 30.5 (br, B−P). ^{11}B NMR (160 MHz, 1,2-$F_2C_6H_4$): δ −0.8 (br), −6.0 (s, BAr^F_4). ESI-MS (1,2-$F_2C_6H_4$) positive ion: *m*/*z* = 629.09 (calcd 629.08, [Rh(dpp3)($C_6H_4F_2$)]$^+$). The weakly bound σ-complex could not be observed.

*Synthesis of [Rh(dpp3)(PR_2H)($H_3B{\cdot}PR_2H$)][BAr^F_4] [R = Adamantyl (**24**)].* Method A follows. To a Youngs flask charged with [Rh(dpp3)(C_6H_5F)][BAr^F_4] (50 mg, 0.034 mmol) and 2 equiv of $H_3B{\cdot}PR_2H$ (**4**) (22 mg, 0.068 mmol) was added 1,2-$F_2C_6H_4$ (5 mL). The solution was stirred at room temperature for 24 h. Complex **24** was isolated as orange solid.

Method B follows. To a Youngs flask charged with [Rh(dpp3)-(C_6H_5F)][BAr^F_4] (50 mg, 0.034 mmol) and 1 equiv of PHR_2 (10 mg, 0.034 mmol) was added 1,2-$F_2C_6H_4$ (5 mL). The solution was stirred for 5 min, and then 1 equiv of $H_3B{\cdot}PR_2H$ (**4**) (11 mg, 0.034 mmol) was added. The solution was stirred for 5 min, and complex **24** was isolated as orange solid (yield 48 mg, 71%). Slow diffusion of pentane (10 mL) into a solution of **24** in 1,2-$F_2C_6H_4$ at −24 °C afforded yellow crystals (one of which was employed for X-ray diffraction studies).

^{1}H NMR (500 MHz, 1,2-$F_2C_6H_4$): δ 8.33 (s, 8 H, BAr^F_4), 7.69 (s, 4 H, BAr^F_4), 3.30 (d, $^1J_{HP}$ = 362 Hz, 1 H, B-PH), 2.87 (d, $^1J_{HP}$ = 412 Hz, 1 H, PH), 2.45−1.56 (66 H, dpp3 CH_2 and adamantyl-H), −0.24 (br, 3 H, BH_3). $^{31}P\{^1H\}$ NMR (202 MHz, 1,2-$F_2C_6H_4$): δ 60.4 (ddd, $J_{PP(trans)}$ = 266 Hz, J_{PRh} = 142 Hz, $J_{PP(cis)}$ = 30 Hz, $Ph_2P(CH_2)_3PPh_2$), 30.5 (s, PHR_2BH_3), 22.8 (dd, J_{PRh} = 163 Hz, $J_{PP(cis)}$ = 30 Hz, $PPh_2(CH_2)_3PPh_2$), 6.6 (ddd, $J_{PP(trans)}$ = 270 Hz, J_{PRh} = 144 Hz, $J_{PP(cis)}$ = 30 Hz, Rh-PR_2BH_3). $^{11}B\{^1H\}$ NMR (160 MHz, 1,2-$F_2C_6H_4$): δ −6.0 (s, BAr^F_4), −42.2 (br, BH_3). ESI-MS (1,2-$F_2C_6H_4$) positive ion: *m*/*z* = 956.30 (unidentified fragment). Anal. Found: C 59.38%, H 4.99%. Calcd for $C_{99}H_{103}B_2F_{24}P_4Rh$: C 59.50%, H 5.20%.

*Synthesis of [Rh(dpp3)H(PCyH·BH_3)($H_3B{\cdot}PCyH_2$)][BAr^F_4] (**25a** and **25b**).* To a Youngs flask charged with [Rh(dpp3)(C_6H_5F)][BAr^F_4] (50 mg, 0.034 mmol) was added 1,2-$F_2C_6H_4$ (5 mL). A 2 equiv portion of $H_3B{\cdot}PH_2Cy$ (**5**) (0.68 mL, 0.1 M solution in 1,2-$F_2C_6H_4$, 0.068 mmol) was then added. The solution was stirred at room temperature for 1 min, and a change in color from orange to pale yellow was observed. Complexes **25a** and **25b** were observed as an approximate 1:1 ratio of isomers and were characterized *in situ* by NMR spectroscopy. Complexes **25a** and **25b** could not be isolated as they reacted quickly to form complexes **26a** and **26b**. The $^{31}P\{^1H\}$ NMR spectrum of this reaction mixture indicates that 2 diastereomers are present; while we were able to identify the 2 sets of 4 resonances each (labeled † and §, based on coupling constants and approximate integrations) it was not possible to determine which set of signals belonged to which diastereomer. See Figure S4, Supporting Information, for more detail.

^{1}H NMR (500 MHz, 1,2-$F_2C_6H_4$): δ 8.32 (s, 8 H, BAr^F_4), 7.69 (s, 4 H, BAr^F_4), 2.73−0.32 (32 H, 3 CH_2 dpp3 + BH_2, CyH, PH), −2.29 (v br, 3 H, BH), −7.92 (br d, 1 H, BH-Rh), −17.51 (s, 1 H, Rh−H). Signals from aromatics not observed due to being overlapped by signals from 1,2-$F_2C_6H_4$. $^{31}P\{^1H\}$ NMR (202 MHz, 1,2-$F_2C_6H_4$): δ

dx.doi.org/10.1021/ic500032f | Inorg. Chem. 2014, 53, 3716−3729

31.7 (dm, J_{PRh} = 134 Hz, $Ph_2P^{1\dagger}(CH_2)_3PPh_2$), 30.5 (dm, J_{PRh} = 129 Hz, $Ph_2P^{1\S}(CH_2)_3PPh_2$), 11.8 (overlapping ddd, $J_{PP(trans)}$ = approximately 200 Hz, J_{PRh} = approximately 104 Hz, $J_{PP(cis)}$ = approximately 25 Hz, $Ph_2P(CH_2)_3P^{2\dagger\S}Ph_2$), −11.0 (br d, $J_{PP(trans)}$ = approximately 200 Hz, Rh-$P^{3\S}$HCy-B), −32.1 (br d, $J_{PP(trans)}$ = approximately 200 Hz, Rh-$P^{3\dagger}$HCy-B), −39.8 (br s, Rh−$H_3BP^{4\dagger}H_2$Cy), −44.2 (br s, Rh−$H_3BP^{4\S}H_2$Cy). ESI-MS (1,2-$F_2C_6H_4$, 60 °C) positive ion: m/z = 747.20 (calcd 747.21, $M^+ - 2BH_3$).

Synthesis of [$(CyH_2P)_2BH_2$]Br. To a stirred solution of $PCyH_2$ (3.40 mL, 10% wt in hexane, 2.0 mmol) in dichloromethane (20 mL) was added $BrH_2B{\cdot}SMe_2$ (1.0 mL, 1.0 M in CH_2Cl_2, 1.0 mmol) and the solution stirred at room temperature for 2 h. The resulting colorless solution was concentrated *in vacuo* to approximately 3 mL, and diethyl ether (30 mL) was added to precipitate a white solid. The solvent was decanted off and the solid washed with a further 10 mL of diethyl ether. The solid was redissolved in dichloromethane, filtered, and recrystallized from a mixture of dichloromethane and diethyl ether at −18 °C to yield white crystals (first crop 0.190 g, second crop 0.041 g, overall yield 71%). At room temperature in CD_2Cl_2 [$(CyH_2P)_2BH_2$]Br undergoes a degenerate exchange reaction; [$(CyH_2P)_2BH_2$]Br is in equilibrium with CyH_2PBH_2Br + PH_2Cy. This exchange process does not occur at −60 °C on the NMR time scale, and each of these species can be observed. In the solid-state the complex exists as [$(CyH_2P)_2BH_2$]Br.

^{1}H NMR (500 MHz, −60 °C, CD_2Cl_2): δ 5.46 (dm, $^1J_{HP}$ = 429 Hz, [$(CyH_2P)_2BH_2]^+$), 4.75 (dm, $^1J_{HP}$ = 388 Hz, CyH_2PBH_2Br), 2.52 (dm, $^1J_{HP}$ = 196 Hz, CyH_2P), 2.37−1.16 (CyH and BH). $^{31}P\{^1H\}$ NMR (202 MHz, −60 °C, CD_2Cl_2): δ −35.5 (br s, [$(CyH_2P)_2BH_2]^+$), −38.2 (br s, CyH_2PBH_2Br), −107.5 (s, CyH_2P). Anal. Found: C 44.35%, H 8.74%. Calcd for $C_{12}H_{28}BBrP_2$: C 44.30%, H 8.68%.

*Synthesis of $CyH_2P{\cdot}BH_2PCyH{\cdot}BH_3$ (**13**).* [$(CyH_2P)_2BH_2$]Br (0.150 g, 0.461 mmol) (prepared as above) and [N^nBu_4][BH_4] (0.119 g, 0.461 mmol) were added to a Schlenk tube. Dichloromethane (10 mL) was added, and effervescence was observed; the solution was stirred at room temperature for 1 h. The solvent was removed *in vacuo*, and *n*-hexane (20 mL) was added to the white solid. The solution was filtered to remove [N^nBu_4]Br and concentrated to approximately 2 mL. Storage of this solution for 16 h at −18 °C yielded colorless crystals of **13** (0.102 g, 86%).

^{1}H NMR (500 MHz, 25 °C, CD_2Cl_2): δ 4.68 (dm, $^1J_{HP}$ = 386 Hz, $CyH_2P{\cdot}BH_2PHCy{\cdot}BH_3$), 3.50 (dm, $^1J_{HP}$ = 326 Hz, $CyH_2P{\cdot}BH_2PHCy{\cdot}BH_3$), 2.17−0.02 (CyH and BH). $^{31}P\{^1H\}$ NMR (202 MHz, 25 °C, CD_2Cl_2): δ −36.6 (br, $CyH_2P{\cdot}BH_2PHCy{\cdot}BH_3$), −45.1 (br, $CyH_2P{\cdot}BH_2PHCy{\cdot}BH_3$). Anal. Found: C 55.79%, H 11.82%. Calcd for $C_{12}H_{30}B_2P_2$: C 55.77%, H 11.71%.

*Synthesis of [Rh(dpp3)H(PHCy·BH_2PHCy·BH_3)][BAr^F_4] (**26a** and **26b**).* Method A follows. To a Youngs flask charged with [Rh(dpp3)(C_6H_5F)][BAr^F_4] (50 mg, 0.034 mmol) was added 1,2-$F_2C_6H_4$ (5 mL) followed by 2 equiv of $H_3B{\cdot}PCyH_2$ (**5**) (0.68 mL, 0.1 M solution in 1,2-$F_2C_6H_4$, 0.068 mmol). The solution was stirred at room temperature for 12 h. The formation of H_2 is also observed. Complexes **26a** and **26b** were characterized as a mixture in solution by NMR spectroscopy and ESI-MS. The $^{31}P\{^1H\}$ NMR spectrum of this reaction mixture indicates that 2 diastereomers are present; we were able to identify the 2 sets of 4 resonances each (labeled **26a** and **26b**, based on coupling constants and approximate integrations) and tentatively assigned the individual diastereomers (Scheme S5, Supporting Information) by inspection of a model.

Method B follows. To a Youngs flask charged with [Rh(dpp3)-(C_6H_5F)][BAr^F_4] (50 mg, 0.034 mmol) and 1 equiv of $CyH_2P{\cdot}BH_2PCyH{\cdot}BH_3$ (**13**) (8.8 mg, 0.034 mmol) was added 1,2-$F_2C_6H_4$ (4 mL). Complexes **26a** and **26b** were characterized as a mixture in solution by NMR spectroscopy and ESI-MS.

^{1}H NMR (500 MHz, 1,2-$F_2C_6H_4$): δ 8.32 (s, 8 H, BAr^F_4), 7.69 (s, 4 H, BAr^F_4), 4.35−3.01 (PH and BH), 2.92−0.92 (30 H, 3CH_2 dpp3, BH_2, CyH), −2.98 (br, 1 H, BH-Rh), −5.98 (br, 1 H, BH-Rh), −16.08 (s, 1 H, Rh−H). Signals from aromatics not observed due to being overlapped by signals from 1,2-$F_2C_6H_4$. $^{31}P\{^1H\}$ NMR (202 MHz, 1,2-$F_2C_6H_4$): δ 37.9 (dm, J_{PRh} = 102 Hz, $Ph_2P^{1b}(CH_2)_3PPh_2$), 34.5 (dm, J_{PRh} = 102 Hz, $Ph_2P^{1a}(CH_2)_3PPh_2$), 19.8 (br d, $J_{PP(trans)}$ = approximately 255 Hz, Rh-P^{3b}HCyB), 16.2 (br d, $J_{PP(trans)}$ = approximately 255 Hz, Rh-P^{3a}HCy-B), 10.7 (overlapping dm, $J_{PP(trans)}$ = 255 Hz, J_{PRh} = 88 Hz, $J_{PP(cis)}$ = approximately 25 Hz, $Ph_2P(CH_2)_3P^{2ab}Ph_2$), −14.9 (br s, Rh-$PHCyBH_2P^{4a}HCyBH_3$), −16.6 (br s, Rh-$PHCyBH_2P^{4b}HCyBH_3$). ESI-MS (1,2-$F_2C_6H_4$, 60 °C) positive ion: m/z = 773.26 (calcd 773.24, M^+).

Synthesis of [Rh(BDPP)(nbd)][BAr^F_4]. [Rh(nbd)$_2$][BAr^F_4] was synthesized by an adaptation of the preparation of [Rh(cod)$_2$]-[BAr^F_4].[63] [Rh(nbd)$_2$][BAr^F_4] (0.100 g, 0.0869 mmol) was dissolved in CH_2Cl_2 (10 mL) to produce a deep red solution. (2*S*,4*S*)-2,4-Bis(diphenylphosphino)pentane (BDPP) (0.0383 g, 0.0869 mmol) was added, and a color change to red was observed. The solution was stirred for 1 h at room temperature before the solvent was removed *in vacuo*. *n*-Pentane (20 mL) was added, and the solution was sonicated to produce an orange powder. The solvent was decanted and the solid washed with pentane (2 × 20 mL). The product was dried *in vacuo* and isolated (yield 0.102 g, 78%).

^{1}H NMR (300 MHz, CD_2Cl_2): δ 7.72 (s, 8 H, BAr^F_4), 7.56 (s, 4 H, BAr^F_4), 7.70−7.36 (m, P-Ph), 4.86 (m, 2 H, =C—H), 4.30 (m, 2 H, =C—H), 3.90 (m, 2 H, nbd C—H), 2.77 (m, 2 H, P—C—H), 1.84 (tt, $^3J_{HH}$ = 6.45 Hz, $^3J_{HP}$ = 19.95 Hz, 2 H, CH_2), 1.58 (m, 2 H, nbd CH_2), 1.13 (m, 6 H, CH_3). $^{31}P\{^1H\}$ NMR (121.6 MHz, CD_2Cl_2): δ 27.4 (d, J_{PRh} = 149 Hz). Anal. Found: C 54.32%, H 3.18%. Calcd for $C_{68}H_{50}BF_{24}P_2Rh$: C 54.47%, H 3.36%.

Synthesis of [Rh(BDPP)(C_6H_5F)][BAr^F_4]. [Rh(BDPP)(nbd)][BAr^F_4] prepared as above (0.020 g, 0.0133 mmol) was added to a high-pressure NMR tube and dissolved in fluorobenzene (0.5 mL). The sample was degassed by the freeze−pump−thaw method and hydrogen gas (4 atm) introduced. The sample was mixed for 30 min and then degassed by the freeze−pump−thaw method and placed under argon.

^{1}H NMR (500 MHz, C_6H_5F): δ 8.32 (s, 8 H, BAr^F_4), 7.61 (s, 4 H, BAr^F_4), 5.63 (m, 2 H, Ar−H), 5.43 (m, 2 H, Ar−H), 5.10 (m, 1 H, Ar−H), 2.38 (m, 2 H, P-CH), 1.40 (m, 2 H, CH_2), 0.78 (m, 6 H, CH_3). Signals from P-Ph not observed due to being overlapped by signals from C_6H_5F. Signals from norbornane (from hydrogenation of norbornadiene) can also be observed at δ 2.12 (m, 2 H, nba C−H), 1.40 (m, 2 H, nba CH_2, overlapped), 1.11 (m, 2 H, nba CH_2). $^{31}P\{^1H\}$ NMR (202 MHz, C_6H_5F): δ 39.9 (d, J_{PRh} = 194 Hz). ESI-MS (C_6H_5F, 60 °C) positive ion: m/z = 639.13 (calcd 639.12, M^+).

*Synthesis of [Rh(BDPP)H($PCyH{\cdot}BH_3$)($H_3B{\cdot}PCyH_2$)][BAr^F_4] (**27a** and **27b**).* [Rh(BDPP)(C_6H_5F)][BAr^F_4] (**26**) was prepared in a high-pressure NMR tube as above. To this was added 2 equiv of $H_3B{\cdot}PH_2Cy$ (**5**) (0.27 mL, 0.1 M solution in 1,2-$F_2C_6H_4$, 0.027 mmol) and the solution mixed for 1 min. Complexes **27a** and **27b** were observed as ratio of isomers and were characterized *in situ* by NMR spectroscopy. Complexes **27a** and **27b** could not be isolated as they reacted quickly to form complexes of **28**; signals for **28** can be observed in both ^{1}H and $^{31}P\{^1H\}$ NMR spectra of **27a** and **27b** which, along with the presence of H_2, show that the complexes rapidly undergo dehydrocoupling to form complexes of **28**. The $^{31}P\{^1H\}$ NMR spectrum of this reaction mixture indicates that 2 diastereomers are present; while we were able to identify the 2 sets of 4 resonances (labeled † and §, based on coupling constants and approximate integrations), it was not possible to determine which set of signals belonged to which diastereomer. See Figure S6, Supporting Information.

^{1}H NMR (500 MHz, C_6H_5F + 1,2-$F_2C_6H_4$): δ 8.32 (s, 8 H, BAr^F_4), 7.69 (s, 4 H, BAr^F_4), 4.19 to 0.32 (CH_3, CH_2, CH, BDPP, BH_2, CyH, PH), −1.80 to −3.31 (v br, 3 H, BH_3), −7.54 to −8.86 (br d, 1 H, BH-Rh), −17.73 (br s, 1 H, Rh−H). Signals from aromatics not observed due to being overlapped by signals from C_6H_5F and 1,2-$F_2C_6H_4$. H_2 can be observed in the NMR spectrum as a sharp singlet at δ 4.52 ppm suggesting that some dehydrocoupling to complex **28** has occurred. This is further evidenced by the small Rh−H hydride signal at δ −16.07 ppm which is observed for complex **28**. $^{31}P\{^1H\}$ NMR (202 MHz, C_6H_5F + 1,2-$F_2C_6H_4$): δ 42.5 (dm, J_{PRh} = 129 Hz, $Ph_2P^{1\dagger}(CH_2)_3PPh_2$), 32.6 (dm, J_{PRh} = 119 Hz, $Ph_2P^{1\S}(CH_2)_3PPh_2$), 28.3 (overlapping ddd, $J_{PP(trans)}$ = approximately 208 Hz, J_{PRh} = approximately 98 Hz, $J_{PP(cis)}$ = approximately 32 Hz, Ph_2P-

dx.doi.org/10.1021/ic500032f | *Inorg. Chem.* 2014, 53, 3716−3729

$(CH_2)_3P^{2\dagger\S}Ph_2$), 3.6 (br d, $J_{PP(trans)}$ = approximately 208 Hz, Rh-$P^{3\S}$HCy-B), −12.1 (br d, $J_{PP(trans)}$ = approximately 208 Hz, Rh-$P^{3\dagger}$HCy-B), −42.1 (br s, Rh−$H_3BP^{4\S}H_2Cy$), −44.2 (br s, Rh−$H_3BP^{4\dagger}H_2Cy$).

*Synthesis of [Rh(BDPP)H(PCyH·BH_2PCyH·BH_3)][BAr^F_4] (**28a**, **28b**, **28c**, and **28d**).* Method A follows. [Rh(BDPP)(C_6H_5F)][BAr^F_4] was prepared on an NMR scale from [Rh(BDPP)(nbd)][BAr^F_4] (0.020 g, 0.0133 mmol) as above. This solution was transferred by cannula to an NMR tube containing $CyH_2P{\cdot}BH_2PHCy{\cdot}BH_3$ (**13**) (3.4 mg, 0.0133 mmol), and the solution was mixed briefly to yield a pale yellow solution.

Method B follows. [Rh(BDPP)(C_6H_5F)][BAr^F_4] was prepared on an NMR scale from [Rh(BDPP)(nbd)][BAr^F_4] (0.020 g, 0.0133 mmol) as above. To this was added 2 equiv of $H_3B{\cdot}PH_2Cy$ (**5**) (0.27 mL, 0.1 M solution in 1,2-$C_6H_4F_2$, 0.027 mmol) and the solution mixed for 18 h.

The $^{31}P\{^1H\}$ NMR spectrum arising from method A indicates that 4 diastereomers are present; while we were able to identify some of the signals from the 4 sets of 4 resonances (labeled †, §, $, and & based on coupling constants and approximate integrations), it was not possible to determine which set of signals belonged to which of the diastereomers. See Figure S7, Supporting Information. Method B affords, essentially, only one diastereoisomer.

^1H NMR (500 MHz, C_6H_5F): δ 8.32 (s, 8 H, BAr^F_4), 7.69 (s, 4 H, BAr^F_4), 5.47−2.46 (PH), 2.11−0.63 (CH, CH_2, and CH_3 BDPP, BH_2, CyH), −3.21 (br, 1 H, BHRh), −5.65 to −6.85 (br, 1 H, BHRh), −16.09, −16.20, and −17.04 (s, 1 H, Rh−H). Signals from aromatics not observed due to being overlapped by signals from C_6H_5F and 1,2-$C_6H_4F_2$. $^{31}P\{^1H\}$ NMR (202 MHz, C_6H_5F): δ 58.9 (ddd, J_{PRh} = 107 Hz, $J_{PP(cis)}$ = 30 Hz, $J_{PP(cis)}$ = 12 Hz, $Ph_2P^{1\S}(CH_2)_3PPh_2$), 58.0 (dm, J_{PRh} = 102 Hz, $Ph_2P^{1\dagger}(CH_2)_3PPh_2$), 46.6 (dm, J_{PRh} = 100 Hz, $Ph_2P^{1\$}(CH_2)_3PPh_2$), 43.6 (dm, J_{PRh} = 102 Hz, $Ph_2P^{1\&}(CH_2)_3PPh_2$), 28.7 (ddd, $J_{PP(trans)}$ = 254 Hz, J_{PRh} = 90 Hz, $J_{PP(cis)}$ = 32 Hz, $Ph_2P(CH_2)_3P^{2\$}Ph_2$), 27.5 (ddd, $J_{PP(trans)}$ = 250 Hz, J_{PRh} = 92 Hz, $J_{PP(cis)}$ = 32 Hz, $Ph_2P(CH_2)_3P^{2\&}Ph_2$), 24.8−17.7 (overlapping m, $J_{PP(trans)}$ = approximately 254 Hz, J_{PRh} = approximately 87 Hz, $J_{PP(cis)}$ = approximately 26 Hz, $Ph_2P(CH_2)_3P^{2\dagger\S}Ph_2$ and Rh-P^3HCy-B), −13.5 to −20.6 (br s of 4 isomers, Rh-PHCyBH_2P^4HCyBH_3). ESI-MS (1,2-$C_6H_4F_2$, 60 °C) positive ion: m/z = 801.29 (calcd 801.29, M^+).

In order to establish that dehydrocoupling had occurred when method B was used to form complexes **28**, excess (10 equiv) of 1,2-bis(diphenylphosphino)ethane was added to the reaction mixture to release the dehydrocoupled product, $CyH_2P{\cdot}BH_2PHCy{\cdot}BH_3$, from the metal center. The $^{31}P\{^1H\}$ NMR spectrum showed two broad signals at δ −37.9 and −43.9 which are in agreement with those found for compound **13**.

Attempted Polymerization of $PhH_2P{\cdot}BH_3$ in Solution. In a procedure similar to that reported by Manners et al.,[20] $PhH_2P{\cdot}BH_3$ (0.248 g, 2.0 mmol) was dissolved in toluene (10 mL) either in the presence of [Rh(dpp3)(C_6H_5F)][BAr^F_4] (14.7 mg, 0.01 mmol) or with no catalyst present. The solution was heated to reflux for 16 h before cooling to room temperature. The solution was concentrated *in vacuo* and added to stirred hexane (100 mL) to produce a white precipitate. The solvent was decanted and the solid washed with hexane (2 × 50 mL). The solid was dried *in vacuo* and isolated in air (yield 0.110 g Rh catalyzed, 0.101 g uncatalyzed). The $^{31}P\{^1H\}$ NMR spectrum of the isolated solids produced by the different methods are very similar with several very broad peaks from δ −45 to −57 and very broad peaks of lower intensity from δ −72 to −87 . See Figure S8, Supporting Information. This is in agreement with the results obtained by Manners et al. for uncatalyzed polymerization of $PhH_2P{\cdot}BH_3$.[20]

Melt Polymerization of $PhH_2P{\cdot}BH_3$. A Youngs flask charged with $PhH_2P{\cdot}BH_3$ (31 mg, 0.25 mmol) and 5 mol % of [Rh(dpp3)(C_6H_5F)][BAr^F_4] (18.4 mg, 0.0125 mmol) was heated to 90 °C for 4 h in melt conditions. The resulting solid was dissolved in 1,2-difluorobenzene and analyzed by NMR spectroscopy. The $^{31}P\{^1H\}$ NMR spectrum shows a peak at δ −49.3 ppm in agreement with that observed by Manners et al.[7] for polymeric material and a lower intensity resonance at δ −55.0 ppm. See Supporting Information Figure S9. In the $^{31}P\{^1H\}$ NMR spectrum the peak at δ −49.3 ppm split into a broad doublet with a J_{PH} coupling constant of approximately 350 Hz. Analysis by ESI-MS of the reaction mixture showed a repeating pattern corresponding to the polymeric repeat unit −[PhHP·BH_2]−, see Figure S10, Supporting Information.

■ ASSOCIATED CONTENT

Ⓢ Supporting Information

Further experimental and characterization details, including selected NMR data and X-ray crystallographic data (including data in CIF format). This material is available free of charge via the Internet at http://pubs.acs.org. Crystallographic data have been deposited with the Cambridge Crystallographic Data Center (CCDC) and can be obtained via www.ccdc.cam.ac.uk/data_request/cif.

■ AUTHOR INFORMATION

Corresponding Author

*E-mail: andrew.weller@chem.ox.ac.uk.

Author Contributions

The manuscript was written through contributions of all authors. All authors have given approval to the final version of the manuscript.

Notes

The authors declare no competing financial interest.

■ ACKNOWLEDGMENTS

The authors acknowledge European Union (FP7, Marie Curie Action "Dehydrocouple"), and the EPSRC (EP/J02127X/1,EP/J020826/1).

■ REFERENCES

(1) Chivers, T.; Manners, I. *Inorganic Rings and Polymers of the p-Block Elements*; RSC: Cambridge, U.K., 2009.

(2) Gauvin, F.; Harrod, J. F.; Woo, H. G. In *Advances in Organometallic Chemistry*; Stone, F. G. A., Robert, W., Eds.; Academic Press: New York, 1998; Vol. *42*.

(3) Jaska, C. A.; Bartole-Scott, A.; Manners, I. *Dalton Trans.* **2003**, 4015−4021.

(4) Reichl, J. A.; Berry, D. H. In *Advances in Organometallic Chemistry*; Robert, W., Anthony, F. H., Eds.; Academic Press: New York, 1998; Vol. *43*.

(5) Clark, T. J.; Lee, K.; Manners, I. *Chem.—Eur. J.* **2006**, *12*, 8634−8648.

(6) Leitao, E. M.; Jurca, T.; Manners, I. *Nat. Chem.* **2013**, *5*, 817−829.

(7) Waterman, R. *Chem. Soc. Rev.* **2013**, *42*, 5629−5641.

(8) Staubitz, A.; Robertson, A. P. M.; Sloan, M. E.; Manners, I. *Chem. Rev.* **2010**, *110*, 4023−4078.

(9) Hamilton, C. W.; Baker, R. T.; Staubitz, A.; Manners, I. *Chem. Soc. Rev.* **2009**, *38*, 279−293.

(10) Staubitz, A.; Robertson, A. P. M.; Manners, I. *Chem. Rev.* **2010**, *110*, 4079−4124.

(11) Wright, W. R. H.; Berkeley, E. R.; Alden, L. R.; Baker, R. T.; Sneddon, L. G. *Chem. Commun.* **2011**, *47*, 3177−3179.

(12) Staubitz, A.; Sloan, M. E.; Robertson, A. P. M.; Friedrich, A.; Schneider, S.; Gates, P. J.; Guànne, J. S.; Manners, I. *J. Am. Chem. Soc.* **2010**, *132*, 13332−13345.

(13) Staubitz, A.; Presa Soto, A.; Manners, I. *Angew. Chem., Int. Ed.* **2008**, *47*, 6212−6215.

(14) Dietrich, B. L.; Goldberg, K. I.; Heinekey, D. M.; Autrey, T.; Linehan, J. C. *Inorg. Chem.* **2008**, *47*, 8583−8585.

(15) Johnson, H. C.; Robertson, A. P. M.; Chaplin, A. B.; Sewell, L. J.; Thompson, A. L.; Haddow, M. F.; Manners, I.; Weller, A. S. *J. Am. Chem. Soc.* **2011**, *133*, 11076−11079.

(16) Dallanegra, R.; Robertson, A. P. M.; Chaplin, A. B.; Manners, I.; Weller, A. S. *Chem. Commun.* **2011**, *47*, 3763−3765.

(17) Baker, R. T.; Gordon, J. C.; Hamilton, C. W.; Henson, N. J.; Lin, P.-H.; Maguire, S.; Murugesu, M.; Scott, B. L.; Smythe, N. C. *J. Am. Chem. Soc.* **2012**, *134*, 5598−5609.
(18) Marziale, A. N.; Friedrich, A.; Klopsch, I.; Drees, M.; Celinski, V. R.; Schmedt auf der Günne, J.; Schneider, S. *J. Am. Chem. Soc.* **2013**, *135*, 13342−13355.
(19) Dorn, H.; Singh, R. A.; Massey, J. A.; Lough, A. J.; Manners, I. *Angew. Chem., Int. Ed.* **1999**, *38*, 3321−3323.
(20) Dorn, H.; Singh, R. A.; Massey, J. A.; Nelson, J. M.; Jaska, C. A.; Lough, A. J.; Manners, I. *J. Am. Chem. Soc.* **2000**, *122*, 6669−6678.
(21) Dorn, H.; Vejzovic, E.; Lough, A. J.; Manners, I. *Inorg. Chem.* **2001**, *40*, 4327−4331.
(22) Friedrich, A.; Drees, M.; Schneider, S. *Chem.—Eur. J.* **2009**, *15*, 10339−10342.
(23) Vance, J. R.; Robertson, A. P. M.; Lee, K.; Manners, I. *Chem.—Eur. J.* **2011**, *17*, 4099−4103.
(24) Sewell, L. J.; Lloyd-Jones, G. C.; Weller, A. S. *J. Am. Chem. Soc.* **2012**, *134*, 3598−3610.
(25) Jaska, C. A.; Manners, I. *J. Am. Chem. Soc.* **2004**, *126*, 9776−9785.
(26) Jaska, C. A.; Dorn, H.; Lough, A. J.; Manners, I. *Chem.—Eur. J.* **2003**, *9*, 271−281.
(27) Jaska, C. A.; Lough, A. J.; Manners, I. *Dalton Trans.* **2005**, 326−331.
(28) Lee, K.; Clark, T. J.; Lough, A. J.; Manners, I. *Dalton Trans.* **2008**, 2732−2740.
(29) Thoms, C.; Marquardt, C.; Timoshkin, A. Y.; Bodensteiner, M.; Scheer, M. *Angew. Chem., Int. Ed.* **2013**, *52*, 5150−5154.
(30) Huertos, M. A.; Weller, A. S. *Chem. Commun.* **2012**, *48*, 7185−7187.
(31) Huertos, M. A.; Weller, A. S. *Chem. Sci.* **2013**, *4*, 1881−1888.
(32) Dorn, H.; Rodezno, J. M.; Brunnhöfer, B.; Rivard, E.; Massey, J. A.; Manners, I. *Macromolecules* **2003**, *36*, 291−297.
(33) Clark, T. J.; Rodezno, J. M.; Clendenning, S. B.; Aouba, S.; Brodersen, P. M.; Lough, A. J.; Ruda, H. E.; Manners, I. *Chem.—Eur. J.* **2005**, *11*, 4526−4534.
(34) Helten, H.; Robertson, A. P. M.; Staubitz, A.; Vance, J. R.; Haddow, M. F.; Manners, I. *Chem.—Eur. J.* **2012**, *18*, 4665−4680.
(35) Helten, H.; Dutta, B.; Vance, J. R.; Sloan, M. E.; Haddow, M. F.; Sproules, S.; Collison, D.; Whittell, G. R.; Lloyd-Jones, G. C.; Manners, I. *Angew. Chem., Int. Ed.* **2013**, *52*, 437−440.
(36) Shuttleworth, T. A.; Huertos, M. A.; Pernik, I.; Young, R. D.; Weller, A. S. *Dalton Trans.* **2013**, *42*, 12917−12925.
(37) McNulty, J.; Zhou, Y. *Tetrahedron Lett.* **2004**, *45*, 407−409.
(38) Van Overschelde, M.; Vervecken, E.; Modha, S. G.; Cogen, S.; Van der Eycken, E.; Van der Eycken, J. *Tetrahedron* **2009**, *65*, 6410−6415.
(39) Eastham, G.; Tindale, N. Catalyst System for Carbonylating Ethylenically Unsaturated Compounds. WO2005079981A1, 2005.
(40) Zapf, A.; Beller, M. *Chem. Commun.* **2005**, 431−440.
(41) Fleckenstein, C. A.; Plenio, H. *Chem. Soc. Rev.* **2010**, *39*, 694−711.
(42) Shimoi, M.; Nagai, S.; Ichikawa, M.; Kawano, Y.; Katoh, K.; Uruichi, M.; Ogino, H. *J. Am. Chem. Soc.* **1999**, *121*, 11704−11712.
(43) Merle, N.; Koicok-Kohn, G.; Mahon, M. F.; Frost, C. G.; Ruggerio, G. D.; Weller, A. S.; Willis, M. C. *Dalton Trans.* **2004**, 3883−3892.
(44) Forster, T. D.; Tuononen, H. M.; Parvez, M.; Roesler, R. *J. Am. Chem. Soc.* **2009**, *131*, 6689−6691.
(45) Spielmann, J.; Piesik, D. F. J.; Harder, S. *Chem.—Eur. J.* **2010**, *16*, 8307−8318.
(46) Kawano, Y.; Yamaguchi, K.; Miyake, S.-y.; Kakizawa, T.; Shimoi, M. *Chem.—Eur. J.* **2007**, *13*, 6920−6931.
(47) Ledger, A. E. W.; Ellul, C. E.; Mahon, M. F.; Williams, J. M. J.; Whittlesey, M. K. *Chem.—Eur. J.* **2011**, *17*, 8704−8713.
(48) Chaplin, A. B.; Weller, A. S. *Angew. Chem., Int. Ed.* **2010**, *49*, 581−584.
(49) Macías, R.; Rath, N. P.; Barton, L. *Angew. Chem., Int. Ed.* **1999**, *38*, 162−164.
(50) Ingleson, M.; Patmore, N. J.; Ruggiero, G. D.; Frost, C. G.; Mahon, M. F.; Willis, M. C.; Weller, A. S. *Organometallics* **2001**, *20*, 4434−4436.
(51) Wagler, J.; Hill, A. F. *Organometallics* **2008**, *27*, 2350−2353.
(52) Nguyen, D. H.; Lauréano, H.; Jugé, S.; Kalck, P.; Daran, J.-C.; Coppel, Y.; Urrutigoity, M.; Gouygou, M. *Organometallics* **2009**, *28*, 6288−6292.
(53) Rablen, P. R. *J. Am. Chem. Soc.* **1997**, *119*, 8350−8360.
(54) Méndez, M.; Cedillo, A. *Comput. Theor. Chem.* **2013**, *1011*, 44−56.
(55) Bellham, P.; Hill, M. S.; Kociok-Kohn, G.; Liptrot, D. J. *Chem. Commun.* **2013**, *49*, 1960−1962.
(56) In principle there should be four diastereoisomers for 25 as both P-centers are stereogenic. However, we assume that the second center (which is next to the BH_3) is far enough removed from the metal center so as not to influence the ^{31}P or ^{1}H chemical shifts significantly.
(57) Wicht, D. K.; Paisner, S. N.; Lew, B. M.; Glueck, D. S.; Yap, G. P. A.; Liable-Sands, L. M.; Rheingold, A. L.; Haar, C. M.; Nolan, S. P. *Organometallics* **1998**, *17*, 652−660.
(58) Robertson, A. P. M.; Leitao, E. M.; Jurca, T.; Haddow, M. F.; Helten, H.; Lloyd-Jones, G. C.; Manners, I. *J. Am. Chem. Soc.* **2013**, *135*, 12670−12683.
(59) Pangborn, A. B.; Giardello, M. A.; Grubbs, R. H.; Rosen, R. K.; Timmers, F. J. *Organometallics* **1996**, *15*, 1518−1520.
(60) Neumann, E.; Pfaltz, A. *Organometallics* **2005**, *24*, 2008−2011.
(61) Schmidbaur, H.; Weiss, E.; Müller, G. *Synth. React. Inorg. Met.-Org. Chem.* **1985**, *15*, 401−413.
(62) Lubben, A. T.; McIndoe, J. S.; Weller, A. S. *Organometallics* **2008**, *27*, 3303−3306.
(63) Guzel, B.; Omary, M. A.; Fackler, J. P., Jr; Akgerman, A. *Inorg. Chim. Acta* **2001**, *325*, 45−50.